

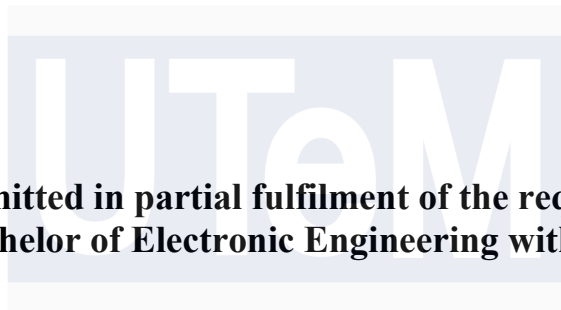
**DEVELOPMENT OF A TISSUE-EQUIVALENT  
PHANTOM FOR TRANSCUTANEOUS ENERGY  
TRANSFER (TET) APPLICATION**



**UNIVERSITI TEKNIKAL MALAYSIA MELAKA**

**DEVELOPMENT OF A TISSUE-EQUIVALENT PHANTOM  
FOR TRANSCUTANEOUS ENERGY TRANSFER (TET)  
APPLICATION**

**NUR AMILIA NADIA BINTI SAMSURI**



**This report is submitted in partial fulfilment of the requirements  
for the degree of Bachelor of Electronic Engineering with Honours**

اونيورسيتي تيكنيكل مليسيا ملاك

**Faculty of Electronics and Computer Technology and  
Engineering  
Universiti Teknikal Malaysia Melaka**

**2025**

BORANG PENGESAHAN STATUS LAPORAN  
PROJEK SARJANA MUDA II

Tajuk Projek : Development of a Tissue-Equivalent Phantom for  
Transcutaneous Energy Transfer (TET) Application  
Sesi Pengajian : 2024/2025

Saya NUR AMILIA NADIA BINTI SAMSURI mengaku membenarkan laporan Projek Sarjana Muda ini disimpan di Perpustakaan dengan syarat-syarat kegunaan seperti berikut:

1. Laporan adalah hakmilik Universiti Teknikal Malaysia Melaka.
2. Perpustakaan dibenarkan membuat salinan untuk tujuan pengajian sahaja.
3. Perpustakaan dibenarkan membuat salinan laporan ini sebagai bahan pertukaran antara institusi pengajian tinggi.
4. Sila tandakan (✓):

**SULIT\***

(Mengandungi maklumat yang berdarjah keselamatan atau kepentingan Malaysia seperti yang termaktub di dalam AKTA RAHSIA RASMI 1972)

**TERHAD\***

(Mengandungi maklumat terhad yang telah ditentukan oleh organisasi/badan di mana penyelidikan dijalankan).

**TIDAK TERHAD**

Disahkan oleh:

\_\_\_\_\_  
(TANDATANGAN PENULIS)

Alamat Tetap:

\_\_\_\_\_  
(COP DAN TANDATANGAN PENYELIA)  
**Ir. Ts. Dr. NOOR BADARIAH BINTI ASAN**  
Pensyarah Kanan

Fakulti Teknologi dan Kejuruteraan Elektronik dan Komputer  
Universiti Teknikal Malaysia Melaka  
Hang Tuah Jaya, 76100 Durian Tunggal, Melaka  
email: noorbadariah@utem.edu.my

Tarikh : 19 Januari 2025

Tarikh : 19 Januari 2025

## DECLARATION

I declare that this report entitled “Development of a Tissue-Equivalent Phantom for Transcutaneous Energy Transfer (TET) Application ” is the result of my own work except for quotes as cited in the references.

اونيورسيتي تيكنيكل مليسيا ملاك  
UNIVERSITI TEKNIKAL MALAYSIA MELAKA

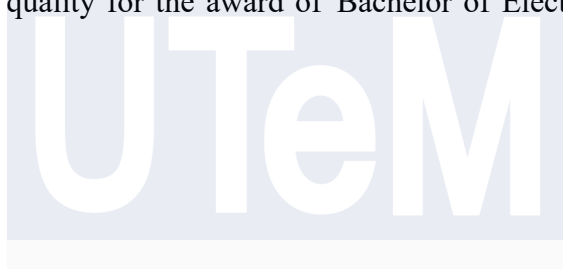
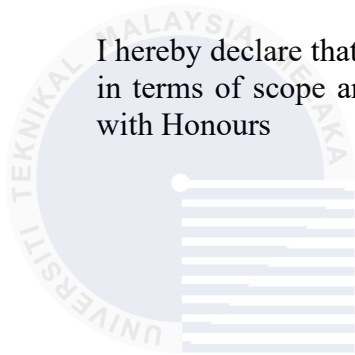
Signature : .....

Author : Nur Amilia Nadia Binti Samsuri

Date : 19 January 2025

## APPROVAL

I hereby declare that I have read this thesis and in my opinion, this thesis is sufficient in terms of scope and quality for the award of Bachelor of Electronic Engineering with Honours



Signature : .....  
اونيورسي تيكنيكل مليسيا ملاك

Supervisor Name : Ir. Ts. Dr. Noor Badariah Binti Asan

Date : 19 January 2025

UNIVERSITI TEKNIKAL MALAYSIA MELAKA

## DEDICATION



You did well dearself....

# UTeM

اونيورسيتي تيكنيكل مليسيا ملاك

UNIVERSITI TEKNIKAL MALAYSIA MELAKA

## ABSTRACT

Transcutaneous energy transfer (TET) has revolutionized the field of medicine by providing a safe and reliable method for powering implants without the need for frequent surgeries to replace batteries. Validating the application of TET using animals is important before human clinical trials. However, these trials contribute to an increased global reliance on animal testing. Currently, there is a lack of research from researchers specifically developing tissue-equivalent phantoms to support TET applications at low frequencies. The goal of this project is to develop and characterize tissue-equivalent phantom materials for TET applications at low frequencies ranging from 1 MHz to 13.56 MHz. The electrical properties of the materials will be measured using an impedance analyzer, and their dielectric properties (permittivity, conductivity, and loss tangent) will be evaluated and compared to human tissues. This research is expected to produce long-lasting, high-fidelity phantom materials that accurately replicate human tissue properties for low-frequency TET applications. This innovation aims to advance research while reducing animal testing in biomedical studies. This structure focuses on motivation, research gaps, objectives, methods, and expected outcomes in a concise and logical manner.

## ABSTRAK

*Sebuah Pemindahan Tenaga Transkutan (TET) telah merevolusikan bidang perubatan dengan menyediakan kaedah yang selamat dan boleh dipercayai untuk memberi tenaga kepada implant tanpa perlu melakukan pembedahan kerap untuk menggantikan bateri. Mengesahkan aplikasi TET menggunakan haiwan adalah penting sebelum ujian klinikal manusia dijalankan. Namun begitu, ujian-ujian ini menyumbang kepada peningkatan kebergantungan global terhadap ujian ke atas haiwan. Pada masa ini, terdapat kekurangan kajian daripada penyelidik khusus untuk membangunkan bahan fantom setara tisu bagi menyokong aplikasi TET pada frekuensi rendah. Matlamat projek ini adalah untuk membangunkan dan mencirikan bahan fantom setara tisu untuk aplikasi TET pada frekuensi rendah antara 1 MHz hingga 13.56 MHz. Sifat elektrik bahan tersebut akan diukur menggunakan penganalisis impedans, dan sifat dielektriknya (permitiviti, konduktiviti, dan kehilangan tangent) akan dinilai serta dibandingkan dengan tisu manusia. Penyelidikan ini dijangka menghasilkan bahan fantom berkualiti tinggi yang meniru sifat tisu manusia untuk aplikasi TET frekuensi rendah. Inovasi ini memajukan penyelidikan sambil mengurangkan ujian haiwan, dengan fokus pada motivasi, jurang, objektif, kaedah, dan hasil secara ringkas dan logik.. .*

## ACKNOWLEDGEMENTS

I would like to express my deepest gratitude to all those who have contributed to the completion of this thesis. First and foremost, I am also thankful to my mother, father, and siblings for their constant encouragement, support, and love. Their support has been my foundation throughout this journey. I would also like to express my gratitude to my supervisor, Ir. Ts. Dr. Noor Badariah Binti Asan, for her invaluable guidance, constructive feedback, and patience throughout the research and thesis writing process. This thesis would not have been possible without her support. Her dedication and expertise have been instrumental in shaping this work. Special thanks go to my housemates and friends who have provided a stimulating and collaborative good environment. Their unwavering support and friendship have been a source of strength and inspiration throughout my academic career. Lastly, I would like to acknowledge all the participants in my study, whose cooperation and contributions were essential for this research. To all of you, I am profoundly grateful.

## TABLE OF CONTENTS

<b>Declaration</b>		
<b>Approval</b>		<b>i</b>
<b>Dedication</b>		<b>i</b>
<b>Abstract</b>		<b>i</b>
<b>Abstrak</b>		<b>ii</b>
<b>Acknowledgements</b>		<b>iii</b>
<b>Table of Contents</b>		<b>iv</b>
<b>List of Figures</b>		<b>viii</b>
<b>List of Tables</b>		<b>x</b>
<b>List of Symbols and Abbreviations</b>		<b>xi</b>
<b>CHAPTER 1 INTRODUCTION</b>		<b>1</b>
1.1 Overview		1
1.2 Problem Statement		2
1.3 Objectives		3

1.4	Scope of Work	4
1.5	Thesis Structure	5
<b>CHAPTER 2 BACKGROUND STUDY</b>		<b>7</b>
2.1	Tissue-Equivalent Phantom	7
2.1.1	Liquid Phantom	8
2.1.2	Solid Phantom	9
2.1.3	Semi-Solid Phantom	9
2.2	Tissue Phantom	9
2.2.1	Skin Tissue	10
2.2.2	Fat Tissue	10
2.2.3	Muscle Tissue	11
2.3	Dielectric Properties	11
2.3.1	Permittivity	11
2.3.2	Conductivity	12
2.3.3	Loss Tangent	13
2.4	State Art of Recent Articles	14
2.5	Dielectric Properties	20
2.6	List of Recipe, Functions and Characteristics	20
2.7	Transcutaneous Energy Transfer (TET)	26
2.7.1	Review Paper of Design and Optimization of Coil for Transcutaneous Energy Transmission System	27

<b>CHAPTER 3 METHODOLOGY</b>	<b>29</b>
3.1 Flowchart of the project	30
3.2 Tissue-Equivalent Phantom Development	32
3.2.1 Development of Skin Tissue-Equivalent Phantom	33
3.2.2 Development of Fat Tissue-Equivalent Phantom	34
3.2.3 Development of Muscle Tissue-Equivalent Phantom	36
3.3 Dielectric Properties Measurement	37
3.3.1 16451B Dielectric Test Fixture Calibration	38
3.3.2 Tissue-Equivalent Phantom Measurement setup	42
3.3.3 Tissue-Equivalent Phantom Measurement Process	43
<b>CHAPTER 4 RESULTS AND DISCUSSION</b>	<b>45</b>
4.1 Results and analysis of Skin Tissue-Equivalent Phantom	46
4.1.1 Recipe of Skin Tissue-Equivalent Phantom	47
4.1.2 Dielectric properties of Skin Tissue-Equivalent Phantom at 1 MHz	48
4.1.3 Dielectric properties of Skin Tissue-Equivalent Phantom at 13.56 MHz	50
4.2 Results and analysis of Fat Tissue-Equivalent Phantom	52
4.2.1 Recipe of Fat Tissue-Equivalent Phantom	52
4.2.2 Dielectric properties of Fat Tissue-Equivalent phantom at 1 MHz and 13.56 MHz	53
4.3 Results and Analysis of Tissue-Equivalent Phantom	55

4.3.1	Recipe for Muscle Tissue-Equivalent Phantom	55
4.3.2	Dielectric properties of Muscle Tissue Phantom at 1MHz	56
4.3.3	Dielectric properties of Muscle Tissue Phantom at 13.56 MHz	58
4.4	Effect of ingredients with the Tissues-Equivalent phantom	61
4.5	Validation Tissue-Equivalent Phantom by using the Transcutaneous Transfer Energy (TET) Application for 1 MHz	66
4.5.1	The Validation Process of Skin, Fat and Muscle Tissue-Equivalent Phantom	68
4.5.2	The Validation process of Skin Tissue-Equivalent Phantom	68
4.5.3	The Validation Process of Fat Tissue-Equivalent Phantom	69
4.5.4	The Validation Process of Muscle Tissue-Equivalent Phantom	70
4.6	Theoretical Validation using Transcutaneous Transfer Energy (TET) Application	72
4.6.1	Skin Tissue phantom (Using Titanium Dioxide sample)	72
4.6.2	Fat Tissue phantom (Using Fat sample F1) & Muscle Tissue phantom (Using Silver powder sample)	74
	<b>CHAPTER 5 CONCLUSION AND FUTURE WORKS</b>	<b>76</b>
5.1	Conclusion	76
5.2	Future Work	78
	<b>REFERENCES</b>	<b>80</b>

## LIST OF FIGURES

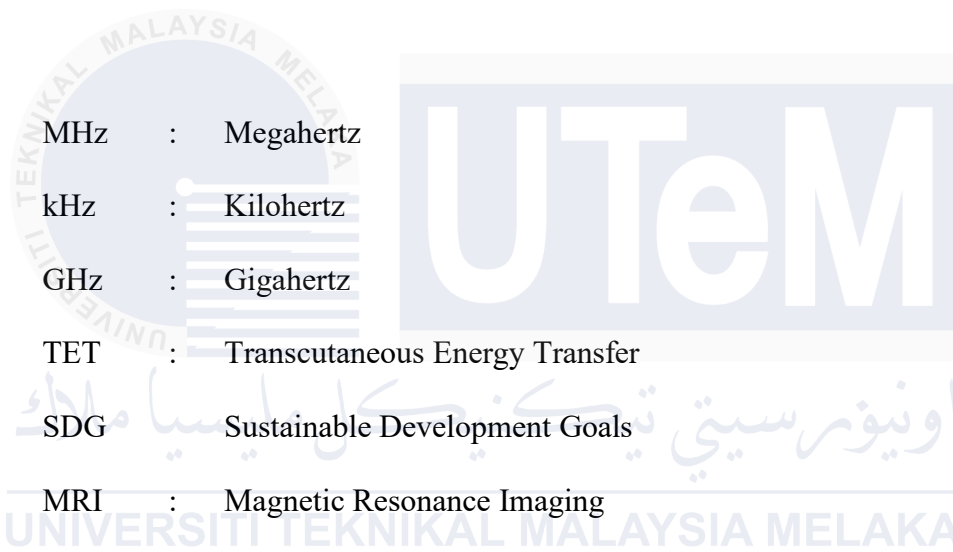
Figure 1.1: Problem Statement	3
Figure 1.2: Scope of Work	4
Figure 2.1: Sample of liquid tissue phantom	8
Figure 2.2: Sample of solid tissue phantom	9
Figure 2.3: Skin Tissue	10
Figure 2.4: Fat Tissue	11
Figure 2.5: Principal of IMD for energy using conductive connection	26
Figure 2.6: Coil temperature measurement experiment by using pork ribs	28
Figure 3.1: Project milestones and flowchart	30
Figure 3.2: Flowchart development of phantom	33
Figure 3.3: Development of Skin tissue phantom	34
Figure 3.4: Development of fat tissue phantom (F1 – Sample 1)	35
Figure 3.5: Development of fat tissue phantom (F2 – Sample 2)	36
Figure 3.6: Development of muscle tissue phantom	37
Figure 3.8: E4990A Impedance Analyzer 20 Hz – 120 MHz	38
Figure 3.9: 165451B Dielectric Test Fixture	38

Figure 3.10: (a) Contact method (vertical position), (b) non-contact method (horizontal position)	39
Figure 3.11: Measurement setup	42
Figure 3.12: Tissue-Equivalent Phantom Measurement Process	43
Figure 4.1: Samples of skin, fat and muscle tissue phantom	46
Figure 4.2: Comparison between permittivity, conductivity and loss tangent for Skin Tissue-Equivalent Phantom Samples at 1 MHz.	49
Figure 4.3: Comparison between permittivity, conductivity and loss tangent for Skin Tissue-Equivalent Phantom Samples at 13.56 MHz.	51
Figure 4.4: Comparison between permittivity, conductivity and loss tangent for Fat Tissue-Equivalent Phantom Samples at 1 MHz and 13.56 MHz.	54
Figure 4.5: Comparison between permittivity, conductivity and loss tangent for Muscle Tissue-Equivalent Phantom Samples at 1 MHz	58
Figure 4.6: Comparison between permittivity, conductivity and loss tangent for Muscle Tissue-Equivalent Phantom Samples at 13.56 MHz	60
Figure 4.7: Permittivity of 4% effect in Skin Tissue Phantom	61
Figure 4.8: Permittivity of 4% effect in Muscle Tissue Phantom	63
Figure 4.9: Permittivity of 8% effect in muscle tissue phantom	64
Figure 4.10: TET Setup	66
Figure 4.11: (a) IV original and (b) ZVS original	67
Figure 4.12: Validation of Skin tissue	69
Figure 4.13: Measurement Results for Skin Tissue (a) IV, (b) ZVS	69
Figure 4.14: Validation of Fat Tissue	70
Figure 4.15: Measurement Results for Fat Tissue (a) IV, (b) ZVS	70
Figure 4.16: Validation of Muscle Tissue	71
Figure 4.17: Measurement Results for Muscle Tissue (a) IV, (b) ZVS	71

## LIST OF TABLES

Table 2.1: Literature review of Tissue-Equivalent Phantoms	14
Table 2.2: Dielectric Properties of 1 MHz	20
Table 2.3: Dielectric Properties of 13.56 MHz	20
Table 2.4: List of the ingredients, functions and characteristics	21
Table 3.1: Calibration steps for E4990A with 16451B [30]	40
Table 4.1: Recipe of Skin Tissue Phantom	47
Table 4.2: Recipe of Fat Tissue Phantom	52
Table 4.3: Recipe of Muscle Tissue Phantom	56
Table 4.4: The study material 4% effect in skin tissue phantom (Permittivity)	61
Table 4.5: The study material 4% effect in muscle tissue phantom (Permittivity)	63
Table 4.6: The study material 8% effect in muscle tissue phantom (Permittivity)	64
Table 4.7: Comparison between Measured and Theoretical Values of Skin	73
Table 4.8: Comparison between Measured and Theoretical Values of Fat	74
Table 4.9: Comparison between Measured and Theoretical Values of Muscle	74

## LIST OF SYMBOLS AND ABBREVIATIONS



MHz	:	Megahertz
kHz	:	Kilohertz
GHz	:	Gigahertz
TET	:	Transcutaneous Energy Transfer
SDG	:	Sustainable Development Goals
MRI	:	Magnetic Resonance Imaging
CT	:	Computed Tomography Scan
TEP		Tissue-Equivalent Phantom
pH		Potential of Hydrogen
IMD		Implanted Medical Device
$\sigma$		Conductivity
$\varepsilon$		Permittivity
$\tan \delta$		Loss Tangent
$\omega$		Angular frequency
$TiO^2$		Titanium Dioxide

# CHAPTER 1



## INTRODUCTION

# UTeM

### 1.1 Overview

Tissue-equivalent phantoms imitate human biological tissues and are crucial for medical research, testing, and device development. Research studies regularly utilize biological tissue-equivalent phantoms, which mimic biological tissue electrical properties (relative permittivity and conductivity) [1]. Tissue equivalent phantoms are used to reduce statistic animal testing worldwide. Most countries' regulations to protect animals from suffering and distress or limit their use are grossly inadequate, despite the large number of animals killed annually in laboratories.

This reduces the number of animals used in experiments, which is ethical and in line with SDG 15 (Life on Land), and reduces the environmental impact of large lab animal populations. Tissue-equivalent phantoms push medical imaging and healthcare technology forward in SDG 3 (Good Health and Well-being). These

phantoms ensure diagnostic reliability and efficiency by testing and calibrating medical equipment like X-ray machines, MRI scanners, and CT scanners. The main goal is to understand these materials' properties, how well they mimic human tissue, and their low-frequency use to 1 MHz and 13.56 MHz. The study will critically evaluate these elements for their effectiveness and durability in phantom development because dielectric properties like permittivity, conductivity, and loss tangent vary across human tissues and rapidly change with frequency.

## 1.2 Problem Statement

Implanted medical devices and measurement testing on animals are rising annually. Before human clinical trials, these initial animal trials are crucial to cyclical design. The involvement of humans in these animal trials ensures medical compliance. People for the Ethical Treatment of Animals (PETA) states, “Every year over 110 million animals including various species like mice, rats, dogs, rabbits and more are killed in US labs for multiple purposes such as research, testing and training” [20].

Thus, tissue-equivalent phantom production and disposal can be more environmentally friendly than animal testing. Development of phantoms that accurately mimic human skin, fat, and muscle is underway. Preclinical assessments using these phantoms will reduce the need for animal subjects in clinical research. Thus, this strategy aims to significantly reduce animal testing in scientific research. The ecological footprint of producing and discarding tissue-equivalent phantoms can be minimized compared to animal research.

Overall, reducing animal killing for testing can benefit the environment by promoting conservation and reducing carbon emissions and pollution. Addressing

that, the main goal of this project is not eliminate animal testing but to control or reduce the need for animal trial usage from statistics animals in the world and to priority the balancing of eco-system that is related to SDG's.

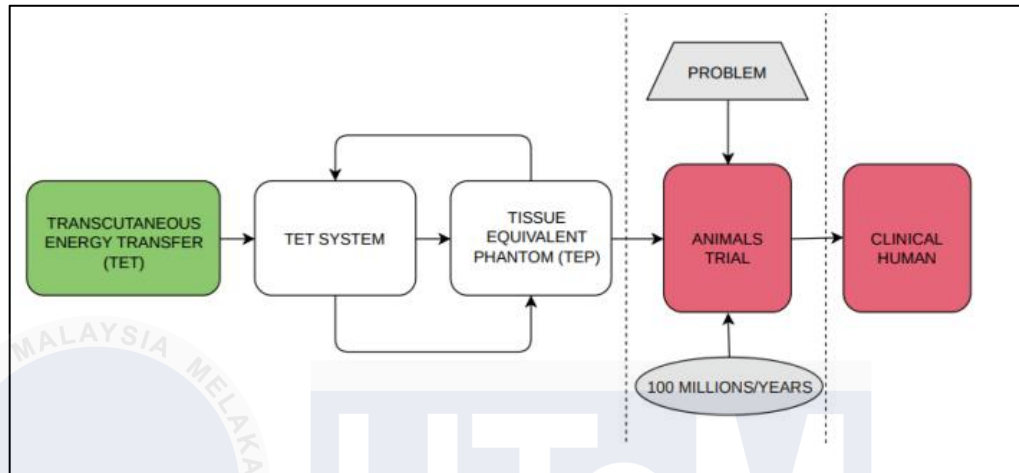


**Figure 1.1: Problem Statement**

### 1.3 Objectives

The project's objectives are as follows,

- To investigate Tissue-Equivalent Phantom materials for Transcutaneous Energy Transfer (TET) Applications.
- To develop the Tissue-Equivalent Phantom at 1 MHz and 13.56 MHz.
- To validate the Tissue-Equivalent Phantom development phantom for Transcutaneous Energy Transfer (TET) Applications.

## 1.4 Scope of Work

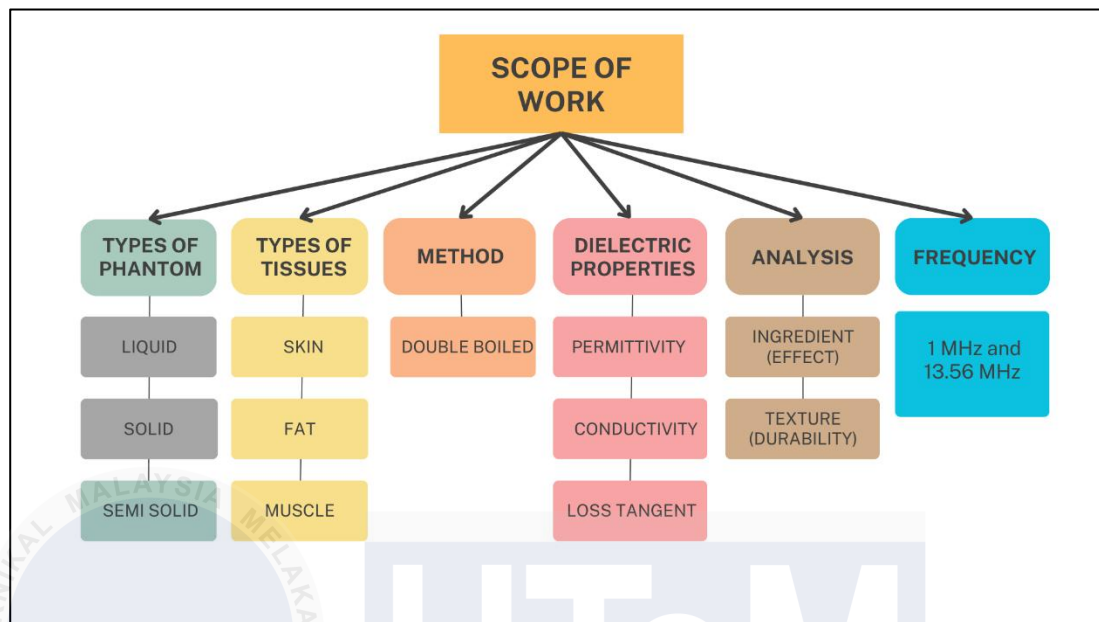


**Figure 1.2: Scope of Work**

Previous studies have established liquid, solid, and semi-solid phantoms to simulate human tissue properties. This project concentrates on semi-solid phantoms, which accurately emulate the characteristics of human tissues such as skin, fat, and muscle. The double boiling technique is frequently employed to produce these phantoms, with its efficacy reliant on the utilization of suitable ingredient formulation. Measurements will be performed in the PSM laboratory to create equivalent phantoms.

The primary objective will also be to assess dielectric properties like permittivity, conductivity, and loss tangent. This measurement must be performed to create tissue-equivalent phantoms, which mimic the electromagnetic properties of human tissue or other substances. This testing is conducted in PERG lab to verify dielectric properties. Although this evaluation of these properties has been done before, this study will focus on how tissue-equivalent phantom development affects its durability.

The development of a tissue-equivalent phantom for transcutaneous energy transfer (TET) requires exploration in the lower frequency spectrum, so the literature review will be limited to 1 MHz and 13.56 MHz. Therefore, the impedance analyzer will be used to measure the material electrical properties.

## 1.5 Thesis Structure

The thesis includes an introduction, background study, methodology, results and discussion, conclusion, and future work. Chapter 1 begins with background research. This background knowledge addresses all project concerns.

Background research for the project was explained in Chapter 2. The dielectric properties of biological tissues, the use of tissue-equivalent phantoms, the procedures to ensure their dielectric properties, and each component used in their development were examined. There was also a background study to identify tissue-equivalent phantom parts and supplies.

Chapter 3 describes project methodology. It begins with a review of recent publications and a dedicated website on project-related topics like tissue phantom types, human tissue dielectric properties (skin, fat, and muscle), frequency-based tissue phantom creation, and applications.

Chapter 4 of this project proposal briefly discusses project results. The developed tissue-equivalent phantom's permittivity, conductivity, and loss tangent will be discussed. Three tissue phantoms were compared for dielectric properties on day 1. In this chapter, phantoms are used to analyze ingredient effects and texture durability.

Chapter 5 concludes by summarizing the research findings and offering important new information and suggestions for sustainability efforts. It discusses research findings and suggests ways to make future projects more sustainable.



## CHAPTER 2



### BACKGROUND STUDY

Chapter 2 highlights the study's literature review, which gathered extensive data for the investigation. Each piece of information will be properly cited from relevant books, articles, scholarly journals, and online sources. The electromagnetic and dielectric properties of the phantom's materials were extensively discussed during composition. The precise formulation of the phantom recipe included selecting materials to accurately mimic human tissue dielectric properties across various frequency ranges.

#### 2.1 Tissue-Equivalent Phantom

Tissue-equivalent phantoms stand as indispensable assets in the progression of medical imaging technologies and the enhancement of patient care. Tissue-equivalent phantoms are vital instruments for developing imaging technologies in

medicine and enhancing patient outcomes. Researchers are still working to improve the precision and dependability of their fabrication techniques [30]. Advanced imaging modalities, such as MRI and CT scans, are often employed to inform the design and validation of these phantoms, ensuring their fidelity to human tissue structures. The development of tissue- equivalent phantoms requires careful attention to multiple factors to guarantee their precision and efficacy in mimicking biological tissues.

### 2.1.1 Liquid Phantom

Liquid phantoms represent specialized entities employed in medical imaging for a multitude of purposes. These phantoms are comprised of homogeneous fluids possessing tailored optical or acoustic properties. In biomedical research, liquid phantoms are indispensable tools, particularly for calibrating and validating medical imaging systems such as ultrasound, CT, and MRI. Their capability to replicate the electromagnetic properties of biological tissues enables precise testing and the development of advanced imaging techniques. The simplest and most flexible to fabricate are liquid tissue phantoms because their volume and consistency are easily regulated and handled [33].

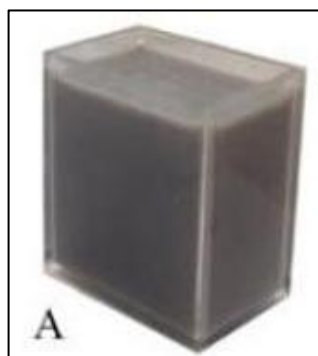


**Figure 2.1: Sample of liquid tissue phantom**

### 2.1.2 Solid Phantom

Solid phantoms serve as reliable test objects that replicate the physical, acoustic, and electromagnetic properties of biological tissues. The composition of solid phantoms is intentionally designed to emulate specific tissue characteristics. The selection of materials is guided by the imaging modality being used and the tissue properties that need to be replicated. Solid phantom samples have been created utilizing bulk matrices such as polymers, silicone, and wax that vary in transparency [33].



**Figure 2.2: Sample of solid tissue phantom**

### 2.1.3 Semi-Solid Phantom

Semi-solid phantoms are designed to mimic the physical and electromagnetic properties of human tissues. These phantoms integrate features of both solid and liquid phantoms, offering a versatile medium for calibrating, validating, and optimizing imaging systems.

## 2.2 Tissue Phantom

Tissue phantoms fundamentally consist of diffuse matrices with diverse compositions, geometries, and optical properties. While they exist in numerous forms, they are typically categorized into solid, hydrogel, and liquid states [33]. Artificial materials designed to mimic the electrical and physical characteristics of human tissues are called tissue phantoms. Especially, phantoms that simulate muscle,

fat, and skin tissues are highly relevant for a variety of therapeutic applications and medical imaging modalities.

### 2.2.1 Skin Tissue

Skin is the outermost layer of the body and serves as a protective barrier. Its dielectric properties vary depending on factors like hydration, thickness, and location. Skin has a relatively high dielectric constant ( $\epsilon$ ) due to its water content. The conductivity ( $\sigma$ ) of skin is low. Skin is composed of three primary visible layers from the surface: the epidermis (100–150 micrometers thick, a blood-free layer), the dermis (1–4 millimeters thick, a vascularized layer), and subcutaneous fat (also known as hypodermis or adipose tissue) (ranging from 1 to 6 millimeters thick, depending on the body site) [34].

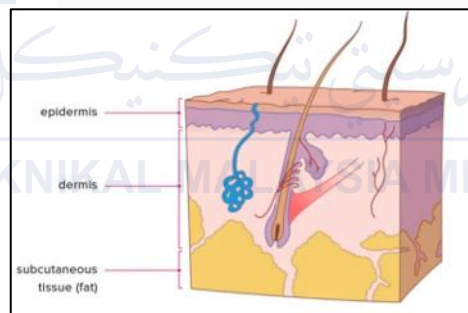


**Figure 2.3: Skin Tissue**

### 2.2.2 Fat Tissue

Fat tissue primarily consists of adipocytes (fat cells) and connective tissue. Its dielectric properties are influenced by lipid content and water content. Fat has moderate dielectric constant and low conductivity. In medical imaging, understanding fat's dielectric properties helps differentiate it from other tissues.

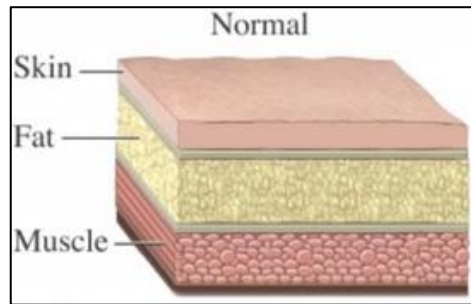


**Figure 2.4: Fat Tissue**

### 2.2.3 Muscle Tissue

Muscle tissue contains muscle fibers, blood vessels, and connective tissue. Its dielectric properties depend on factors like muscle type (skeletal, cardiac, or smooth) and hydration. Muscles have a higher dielectric constant than fat but lower than skin. Its conductivity is moderate. Muscle stands as one of the most abundant tissues in the human body, and understanding its optical properties holds significant importance for both therapeutic and diagnostic applications [34].

## 2.3 Dielectric Properties

The permittivity, conductivity, and loss tangent are important in electromagnetic interactions, especially in tissue phantoms used in medicine and technology. For realistic dielectric properties across frequency ranges, materials must be carefully selected and combined to match human tissues. Continuous research improves measurement methods and computational models to validate and optimize tissue equivalent phantom dielectric properties for reliability and accuracy in medical and technological applications.

### 2.3.1 Permittivity

Permittivity ( $\epsilon$ ), also referred to as relative permittivity or dielectric constant, assesses a material's capacity to store electrical energy within an electric field, measuring its polarization in response to applied electrical stimuli. In the realm of

tissue phantoms, permittivity governs the fidelity with which the phantom replicates the electrical characteristics of human tissues. Diverse tissue types exhibit disparate permittivity values owing to distinctions in their molecular makeup and structural arrangements.

Permittivity, denoted by  $\epsilon$ , is a fundamental property of dielectric materials. It characterizes how well a material can store electrical energy when subjected to an electric field. The permittivity can be real or complex, depending on the presence of loss mechanisms (such as conductivity or dielectric relaxation). It is generally expressed as a complex quantity:

$$\epsilon = \epsilon' - j\epsilon'' \quad (2.1)$$

Where:

- $\epsilon'$  is the real part of the permittivity (dielectric constant).
- $\epsilon''$  is the imaginary part of the permittivity (dielectric loss).

### 2.3.2 Conductivity

Conductivity ( $\sigma$ ) measures a material's ability to conduct electrical current. It quantifies the ease with which charge carriers (e.g., ions or electrons) can move through the material in response to an electric field. In biological tissues, conductivity arises from the presence of electrolytes (e.g., ions dissolved in bodily fluids) and varies depending on factors such as tissue type, hydration level, and temperature. The conductivity of a material is related to the imaginary part of the permittivity and the angular frequency ( $\omega$ ) of the applied electric field. It is given by:

$$\sigma = \omega\epsilon_0\epsilon'' \quad (2.2)$$

Where:

- $\sigma$  is the electrical conductivity.
- $\omega$  is the angular frequency ( $\omega = 2\pi f$ , where  $f$  is the frequency)
- $\epsilon_0$  is the permittivity of free space ( $\approx 8.854 \times 10^{-12} \text{F/m}$ )
- $\epsilon''$  is the imaginary part of the permittivity.

### 2.3.3 Loss Tangent

The loss tangent ( $\tan \delta$ ), also known as the loss factor or dissipation factor, quantifies the energy dissipation in a dielectric material when subjected to an alternating electric field. It represents the ratio of the imaginary part of the permittivity (related to energy loss) to the real part of the permittivity (related to energy storage). In tissues, factors such as ion mobility, molecular rotation, and tissue microstructure contribute to dielectric losses. Higher loss tangent values indicate greater energy dissipation and are associated with increased tissue absorption and heating in electromagnetic fields. It offers an alternative approach to quantify the impact of loss on the electromagnetic field within a material [32]. Loss tangent is defined as the ratio of the imaginary part of the complex permittivity ( $\epsilon''$ ) to the real part of the complex permittivity ( $\epsilon'$ ). Mathematically, it is expressed as:

$$\text{Loss Tangent, } \tan \delta = \frac{\epsilon''}{\epsilon'} \quad (2.3)$$

In essence, comprehending and faithfully reproducing the dielectric properties of biological tissues within tissue phantoms encompassing parameters like permittivity, conductivity, and loss tangent are critical for simulating authentic electromagnetic responses. This is pivotal in guaranteeing the efficacy and safety of medical and technological devices and procedures.

## 2.4 State Art of Recent Articles

Table 2.1 below shows the literature review of state tissue-equivalent phantoms from the previous paper:

**Table 2.1: Literature review of Tissue-Equivalent Phantoms**

Ref.	Title	State of phantom	Types of Tissue	Frequency	Aim	Ingredients	Measurement
[1]	Development of multi-layered biological tissue-equivalent phantom for HF band (Ryotaro Suga, 2013)	Semi-solid	Muscle, skin and Fat	21 MHz	To investigate the interaction between electromagnetic waves and human body in the high frequency (HF) band.	<ul style="list-style-type: none"> <li>• Deionized water</li> <li>• Agar Powder</li> <li>• Aluminium Powder</li> <li>• Sodium Chloride</li> </ul>	Impedence Analyzer (6530B, Wayne Kerr Electronic)
[2]	Development of 500 kHz	Solid	Muscle	500 kHz	To develop tissue	<ul style="list-style-type: none"> <li>• Ionized water</li> </ul>	6530B LCR

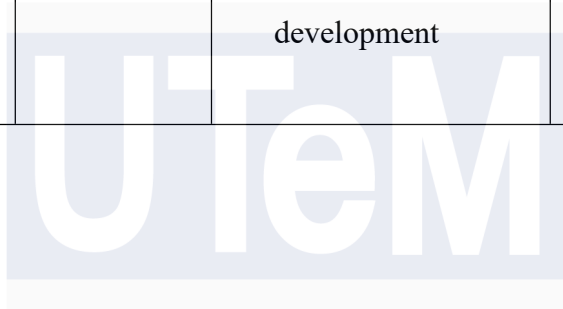
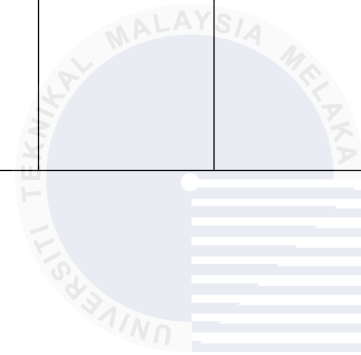
	muscle equivalent solid phantom (Aditya Rakhmadi, 2020)				mimicking phantom that mimics the dielectric properties of human muscle at frequency of 500kHz	<ul style="list-style-type: none"> <li>Aluminium Powder</li> <li>Gellan gum</li> </ul>	Meter (Wayne Kerr Electronics, Sussex, UK)
[3]	Development of muscle-equivalent phantom for electrical impedance tomography (Seiya Toyoda, 2022)	Solid	Muscle	10 kHz – 10 MHz	Making specific material changes to mimic human body properties over a wide frequency band achieving accuracy in electrical properties for frequency range.	<ul style="list-style-type: none"> <li>Polyethylene powder (PEP)</li> <li>Glycerol</li> <li>Titanium dioxide coated with antimony-doped tin oxide (ATO/TiO<sub>2</sub>)</li> </ul>	Not mentioned
[4]	Temperature dependence	Semi-Solid	Breast	50 MHz to	Tissue mimicking	<ul style="list-style-type: none"> <li>Distilled water</li> </ul>	Open-ended

	studies of tissue mimicking phantoms for ultra-wideband microwave breast tumor (T. Slanina, 2022)			20 GHz	phantoms modelling the temperature dependent dielectric properties of breast tissue over large frequency	<ul style="list-style-type: none"> <li>• Glycerin</li> <li>• Agar-agar</li> <li>• Rapeseed oil</li> <li>• Dishwashing liquid</li> </ul>	coaxial probe and network analyzer
[5]	Tissue phantoms to mimic the dielectric properties human forearm phantom section for multi-frequency bioimpedance analysis at low frequencies.	Semi-Solid	Fat, Muscle, Blood	1 kHz to 2 MHz	Developing human forearm phantoms specifically to exhibit the dielectric properties of fat, muscle, and blood tissue	<ul style="list-style-type: none"> <li>• Propylene glycol</li> <li>• Saline solution</li> <li>• Agar-agar</li> <li>• Gelatin</li> </ul>	Quadra Impedance Spectroscopy device (Cole model)
[6]	A tissue equivalent	Semi-solid	Muscle, Fat,	902 to 928	Tissue equivalent	<ul style="list-style-type: none"> <li>• Diethylene</li> </ul>	<ul style="list-style-type: none"> <li>• 85070B</li> </ul>

	phantom of the human torso for in vivo biocommunications (David M. Peterson, 2010)		Bone	MHz	(TEQ) was designed and constructed for Vivo biocompatible communication systems operating	Glycol (DEG) <ul style="list-style-type: none"> <li>• Distilled water</li> <li>• NaCl</li> <li>• TX-151</li> <li>• Polysaccharide gel</li> </ul>	Dielectric probe kit with software <ul style="list-style-type: none"> <li>• HP8752A vector network software</li> </ul>
[7]	Theoretical and experimental broadband tissue equivalent phantoms at microwave and millimetre-wave frequencies	Semi-solid	Muscle	26.5 to 40 GHz	Fabricate tissue equivalent phantoms for reflection measurements, introduce novel composition for low-	<ul style="list-style-type: none"> <li>• DI water</li> <li>• Agar-agar</li> <li>• PE powder</li> <li>• Guar gum</li> <li>• Gelatin</li> </ul>	<ul style="list-style-type: none"> <li>• Agilent E8361C vector network analyzer VNA</li> </ul>

	(R. Aminzadeh, 2014)				cost phantom		<ul style="list-style-type: none"> <li>• Agilent 85070 software</li> </ul>
[8]	Biological tissue equivalent phantoms usable in broadband frequency range (2007)	Liquid and Solid	Brain, Muscle	3 to 10 GHz	To discuss the use of biological tissue equivalent phantom in evaluating absorption of electromagnetic energy and antenna characteristics near human body	<ul style="list-style-type: none"> <li>• DI water</li> <li>• Agar Powder</li> <li>• NaCl</li> <li>• Sodium dehydroacetate</li> <li>• TX-151</li> <li>• Polyethylene powder (PEP)</li> </ul>	Not Mentioned
	Development of a tissue-equivalent phantom for	Semi-Solid	Skin, Fat, Muscle	1 MHz and 13.56 MHz	<ul style="list-style-type: none"> <li>• Low frequencies</li> <li>• To analyze the</li> </ul>	React especially in low frequencies	E4990A Impedance

	Transcutaneous Energy (TET) Application (Purposed)				effect of the tissue- equivalent phantom development	that mimic the tissue-equivalent phantom	Analyzer (20 Hz – 120 MHz)
--	--	--	--	--	--	--	-------------------------------



اونيورسيتي تيكنيكل مليسيا ملاك  
UNIVERSITI TEKNIKAL MALAYSIA MELAKA

## 2.5 Dielectric Properties

Tables 2.2 and 2.3 show skin, fat, and muscle dielectric properties at 1 MHz and 13.56 MHz. Researchers studying the interactions of electromagnetic (EM) fields and biological systems often demand extensive data on human tissue dielectric properties [31]. The Italian National Research Council website published data from 1997 to 2024 using a parametric model to calculate body tissue dielectric properties [21].

**Table 2.2: Dielectric Properties of 1 MHz**

Tissues	Permittivity	Conductivity (S/m)	Loss Tangent
Skin (Wet)	1832.8	0.2214	2.1715
Fat	27.222	0.025079	16.56
Muscle	1836.4	0.50268	4.9204

**Table 2.3: Dielectric Properties of 13.56 MHz**

Tissues	Permittivity	Conductivity (S/m)	Loss Tangent
Skin (Wet)	177.13	0.38421	2.8754
Fat	11.827	0.030354	3.4021
Muscle	138.44	0.62818	6.0152

## 2.6 List of Recipe, Functions and Characteristics

Table 2.4 below shows the lists of the ingredients, functions and characteristics that are used to develop tissue-equivalent phantoms.

**Table 2.4: List of the ingredients, functions and characteristics**

<b>Ingredients</b>	<b>Functions</b>	<b>Characteristics</b>
Distilled water	Acts as a solvent and provides a base medium for the mixture.	Pure water devoid of contaminants, ensuring uniformity and standardization in recipes.
Silicone Emulsion	Used as a lubricant and releasing agent.	It is a water-based non-ionic system with good stability and dilution.
Aluminium Powder	Adjust relative permittivity of phantom [2]	Fine metallic powder that enhances X-ray attenuation, allowing the phantom to simulate bone structures in imaging.
Glycerin	As a softening agent and humectant and helps to maintain moisture.	A clear, viscous liquid that maintains the moisture content and pliability of the phantom.
Cooking oil	This vegetable oil boasts low saturated fat content while offering high levels of monounsaturated and polyunsaturated fats. It is abundant in omega-3 fatty acids and exhibits a high smoke point.	A viscous, hydrophobic liquid that provides the necessary lipid-like properties to the phantom.

PDV Salts	These salts may be used to adjust the pH.	High-purity salt that dissolves easily, replicating the ionic environment of biological tissues.
Polyvinylpyrrolidone/ PVP Powder	PVP is a polymer that can help to control the mechanical properties.	A water-soluble polymer that forms a gel-like consistency, contributing to the phantom's texture.
Gelatin	Commonly used to simulate soft tissue in phantoms due to its similar mechanical properties	A protein-based, thermoreversible gel that mimics the texture and consistency of soft tissues.
Agar-Agar Powder	Agar stabilizes oil droplets, producing gels with smaller (10-21 $\mu$ m) and more uniform oil droplets [22]	A polysaccharide that forms firm gels, often used for its biocompatibility and ability to replicate soft tissue firmness.
Japanese Agar-Agar Powder	A gelatinous substance extracted from seaweed, and it may be used as a gelling agent.	Similar to standard agar-agar but often purer, forming more consistent and firm gels.
Sodium Alginate	Gelling agent that can be used to create a gel-like consistency.	A polysaccharide that creates strong, stable gels.
Carrageenan Powder	Carrageenan is a polysaccharide extracted from red seaweed and is used as a thickening agent and gelling	A sulfated polysaccharide that forms various gel textures, mimicking the consistency of soft tissues.

	agent in the phantom.	
Sodium Benzoate	As a preservative to prevent microbial growth.	An antimicrobial agent ensuring the longevity of the phantom by inhibiting bacterial and fungal growth.
Guar Gum	Thickening agents that can be used to adjust the viscosity.	A high-viscosity polysaccharide that forms thick, stable gels, enhancing the texture of the phantom.
Sodium Percarbonate	Used as a bleaching agent or to provide oxygen release in the phantom.	Releases hydrogen peroxide upon dissolution, used for its oxidative and cleaning properties.
Hydroxyethyl Cellulose	Thickening agent and may also contribute to the overall mechanical properties	A non-ionic, water-soluble polymer that increases viscosity and stabilizes emulsions.
Maltodextrin	Carbohydrates are often used as a bulking agent or sweetener. In this context, it may contribute to the overall composition of the phantom.	An easily digestible carbohydrate that provides structure without significant sweetness, enhancing the bulk and texture.
Xanthan Gum	Thickening agents that can be used to adjust the viscosity.	A high-viscosity polysaccharide that forms stable gels and exhibits shear-thinning properties, important for mimicking

		the flow properties of biological tissues.
Sodium Citrate	Used as a buffer to control the Ph.	The sodium salt of citric acid, used to maintain a stable pH and act as an anticoagulant.
Polyethylene Powder	Adjust the density of the phantom	An inert polymer powder that provides mechanical strength and stability to the phantom.
Polyvinylpyrrolidone (PVP40-50g)	It forms hydrogels resembling soft tissue texture, is biocompatible, and allows precise tuning of mechanical properties like elasticity and stiffness.	A higher molecular weight PVP that forms more robust gels, contributing to the phantom's viscosity and structural integrity.
Polyethylene	As a structural component in the phantom or to adjust its mechanical properties.	A durable polymer is used for its mechanical properties and stability, adding rigidity where needed.
Ethanol	Used as a solvent or to adjust the drying time.	A volatile organic solvent that serves as an antibacterial to keep impurities out of the combination.
Gellan Gum	Used to solidified phantom (has minimal effect on the change of phantom dielectric properties) [2]	forms a gel-like substance when mixed with water.

Soy Lecithin	An emulsifier to help disperse ingredients evenly throughout the phantom.	Soy lecithin is a natural emulsifier derived from soybeans. It contains phospholipids and fatty acids.
Sodium Chloride	Used to adjust the conductivity of the phantom to mimic that of human tissue.	Common table salt.
Titanium Dioxide (TiO <sub>2</sub> )	Has high dielectric properties and can be used to increase the dielectric permittivity in composites	Light scattering and opacity enhancement.
Activated Carbon / Charcoal Powder	Absorption and light attenuation.	High surface area, excellent adsorbent, black pigment.

Once the materials most used for crafting the tissue-equivalent phantom are identified, the subsequent step involves pinpointing the most efficient recipe based on the ingredients list. This entails mixing materials to achieve the desired structure, dielectric properties, physical texture, and other specifications. It's crucial to note that even minor adjustments to the recipe could substantially alter the dielectric characteristics of the tissue-equivalent phantoms, which are paramount to the outcome.

## 2.7 Transcutaneous Energy Transfer (TET)

Transcutaneous Energy Transfer (TET) is a method used to wirelessly transmit power across a barrier, typically through the skin. An alternating magnetic field generates a subcutaneous electric current, which then transmits electrical energy to the implanted medical device (IMD) [35].

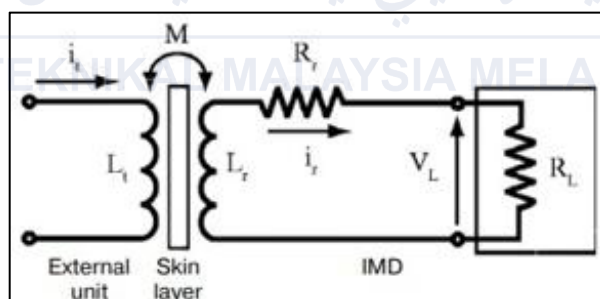


**Figure 2.5: Principal of IMD for energy using conductive connection**

Basic Principles of Transcutaneous Transfer Energy (TET):

- 1) Electromagnetic Induction: TET relies fundamentally on electromagnetic induction, where a changing magnetic field within a coil of wire induces an electric current in a nearby coil. This is the same principle used in wireless charging for electronic devices.

- 2) **Primary and Secondary Coils:** Tet systems typically comprise two key components which a primary coil (transmitter) positioned outside the body and a secondary coil (receiver) implanted inside the body near the skin. When an alternating current (AC) flows through the primary coil, it generates a magnetic field.
- 3) **Magnetic Coupling:** The magnetic field from the primary coil penetrates the skin and induces an electric current in the secondary coil. This process, known as magnetic coupling, depends on the alignment, distance between the coils, and the frequency of the AC in the primary coil for efficient energy transfer.
- 4) **Power Conversion:** The induced current in the secondary coil is converted into a usable form of power for the implanted device. This typically involves converting AC to DC (rectification) and regulating the voltage to meet the device's power requirements.

#### **—2.7.1— Review Paper of Design and Optimization of Coil for Transcutaneous Energy Transmission System**

The research paper titled "Design and Optimization of Coil for Transcutaneous Energy Transmission System" is by H. H. Hoang, N. V. Pham, V. T. Duong, and Q. T. Nguyen. Presents a comprehensive study focused on enhancing the efficiency and effectiveness of coils used in transcutaneous energy transmission systems (TETS). The authors delve into various design parameters and optimization techniques to improve power transfer efficiency and reduce energy losses, which are critical for medical applications such as powering implanted medical devices. Through a series of simulations and experimental validations, the paper investigates the impact of coil geometry, material selection, and coupling efficiency on the overall performance of the system. The findings indicate that optimizing the coil design not only enhances the

power transfer capability but also minimizes heat generation, which is crucial for patient safety and comfort. Additionally, the paper explores advanced optimization algorithms to identify the best configurations, offering valuable insights into the practical implementation of TETS. This research significantly contributes to the field by providing a detailed analysis and practical guidelines for designing more efficient and reliable energy transmission systems in medical applications.

The application of the research on the design and optimization of coils for transcutaneous energy transmission systems (TETS) primarily lies in the medical field, particularly in powering implantable medical devices. These devices include cardiac pacemakers, cochlear implants, and neurostimulators, which are critical for maintaining and enhancing the quality of life for patients with various health conditions. The paper's focus on optimizing coil design is crucial because the efficiency of power transfer directly impacts the reliability and longevity of the implanted devices. By improving the coil's design, the researchers aim to maximize power transfer efficiency, ensuring that sufficient energy is delivered to the implant with minimal losses.

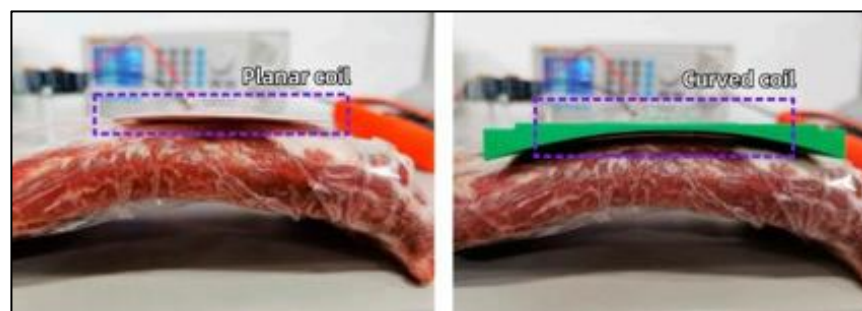
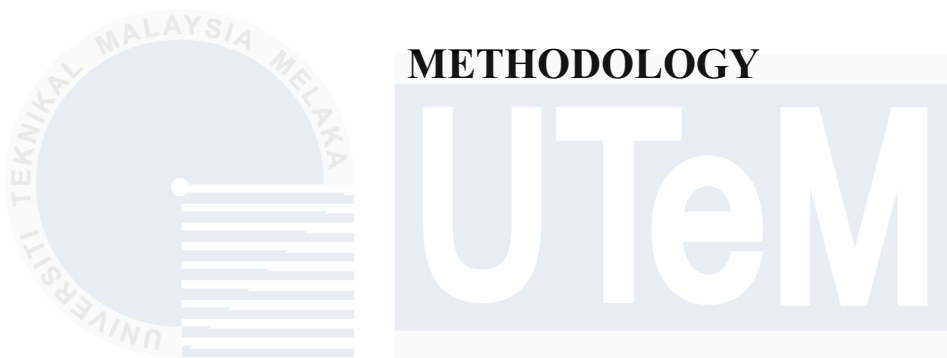


**Figure 2.6: Coil temperature measurement experiment by using pork ribs**

## CHAPTER 3



اونيورسيتي تيكنيكل مليسيا ملاك

Chapter 3 will outline the entire process of developing and accessing tissue-equivalent phantom materials for Transcutaneous Energy Transfer (TET) applications. It provides a concise overview of the research methodology, including details on the flowchart of the project, preparation, development of the tissue-equivalent phantom method, and measurement of the phantom's dielectric properties. Additionally, it discusses the production of the necessary ingredients for manufacturing, and the formulation of the phantom recipe based on literature research.

### 3.1 Flowchart of the project

Figure 3.1 below shows the flowchart for Development of a Tissue-Equivalent Phantom for Transcutaneous Energy Transfer (TET) Application:

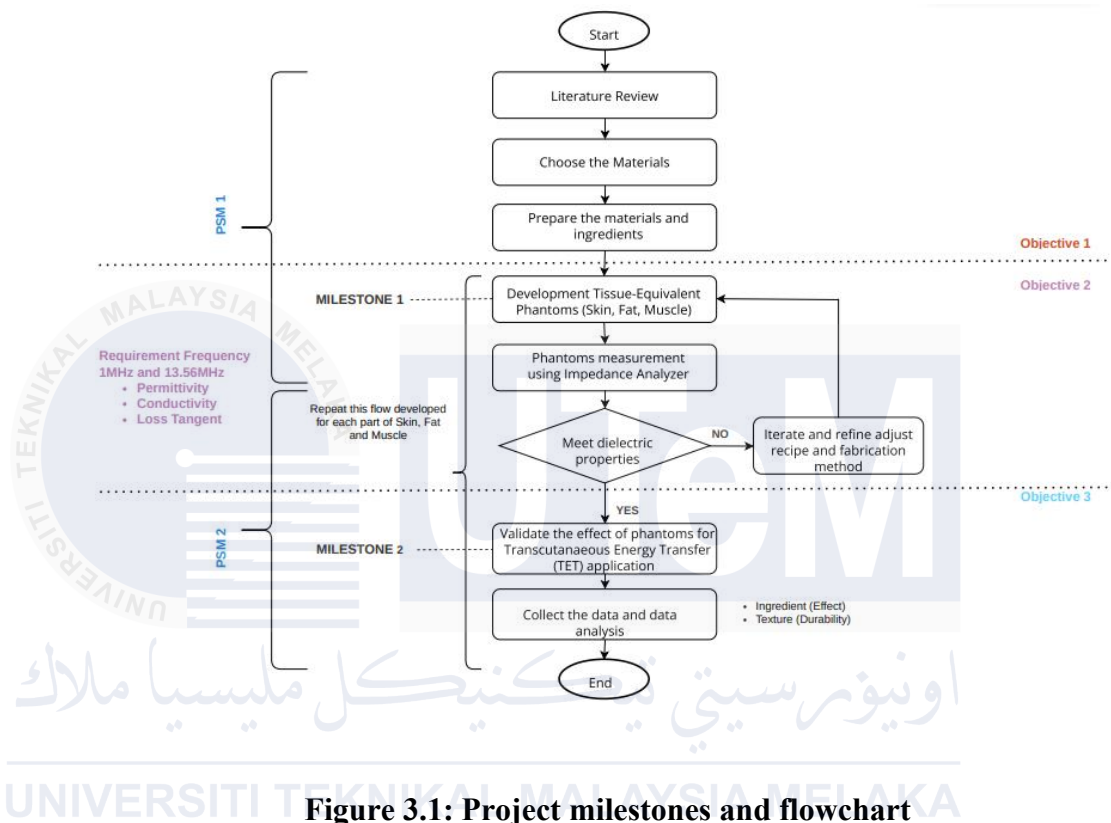


**Figure 3.1: Project milestones and flowchart**

To create a material that can replicate human tissue's characteristics, such as fat, skin, and muscle, for a variety of purposes, phantom tissue creation entails several procedures. Before creating tissue-equivalent phantoms, start by conducting a thorough literature review by exploring existing studies and research related to these phantoms. This step helps to understand the current state of knowledge, available materials, and techniques used in the field. Based on the insights gained from the literature review, then select appropriate materials. These materials should closely mimic the dielectric properties of human tissues. Factors like permittivity (how well a material can store electrical energy), conductivity (ability to conduct electricity), and loss tangent (dissipation of energy) are considered. Common materials include

water- based gels, polymers, and other tissue-mimicking substances. Once the materials are chosen, prepare them according to specific recipes. This involves mixing and processing to achieve the desired properties. Ingredients may include water, gelatin, or other components that simulate tissue behavior. So, this achieves objective 1 that involves investigating tissue-equivalent phantom materials for Transcutaneous Energy Transfer (TET) Applications.

Once the most effective phantom recipe has been discovered, the following step is to develop the tissue-equivalent phantom which has three tissues: skin, muscle and fat. During this stage, several sorts of phantoms will be produced simply by modifying the amount of ingredients in the formula. Upon successfully fabricating the tissue phantoms, the following step is to calibrate the Impedance Analyzer, which is used to measure the electrical properties of material. The characteristics of dielectric properties such as permittivity, conductivity, and loss tangent will be proved during the measurement by comparing them to the dielectric properties of human tissues. The derived tissue phantom samples were maintained in a chemical refrigerator to prevent mold formation and to monitor the changes in the dielectric properties over time. Adjust the phantom properties as needed to match the desired dielectric properties. This refinement process includes tweaking the recipe and fabrication method by iterating this step for each part of the phantom. In short, this archives the second objective which focuses on developing the tissue-equivalent phantom at 1 MHz and 13.56 MHz. It creates tissue-equivalent phantoms using the chosen materials and measurements are taken at specific frequencies 1 MHz and 13.56 MHz to ensure the phantoms exhibit the desired electrical behavior.

The third objective is critical for assessing the effectiveness of these phantoms in Transcutaneous Transfer Energy (TET) applications by validating whether the phantoms accurately simulate human tissues in terms of electrical properties. Additional data related in terms of the analysis by the effect of ingredients and the durability of the phantoms are collected during this validation process.

### 3.2 Tissue-Equivalent Phantom Development

The development of tissue-equivalent phantoms is a critical area of research and application in medical physics, particularly in medical imaging, radiation therapy, and dosimetry. These phantoms are designed to simulate human tissue properties as closely as possible, both in terms of physical characteristics (like density and elasticity).

Figure 3.2 illustrates the flowchart how to develop a phantom, starting with a literature review to determine ingredient composition. Based on previous studies, this step ensures rational material selection. Following identification, the ingredients are measured and weighed for precise proportions. To optimize mixing, water is double boiled heated at 60°C to 80°C. A beaker is used to mix the pre-measured ingredients with the heated water for a uniform mixture. After mixing, the phantom cools slowly to stabilize its physical and chemical properties. Finally, the cooled phantom is stored properly to maintain its quality and usability. Each step of this detailed process ensures accuracy, consistency, and proper handling, producing a high-quality phantom for various applications.

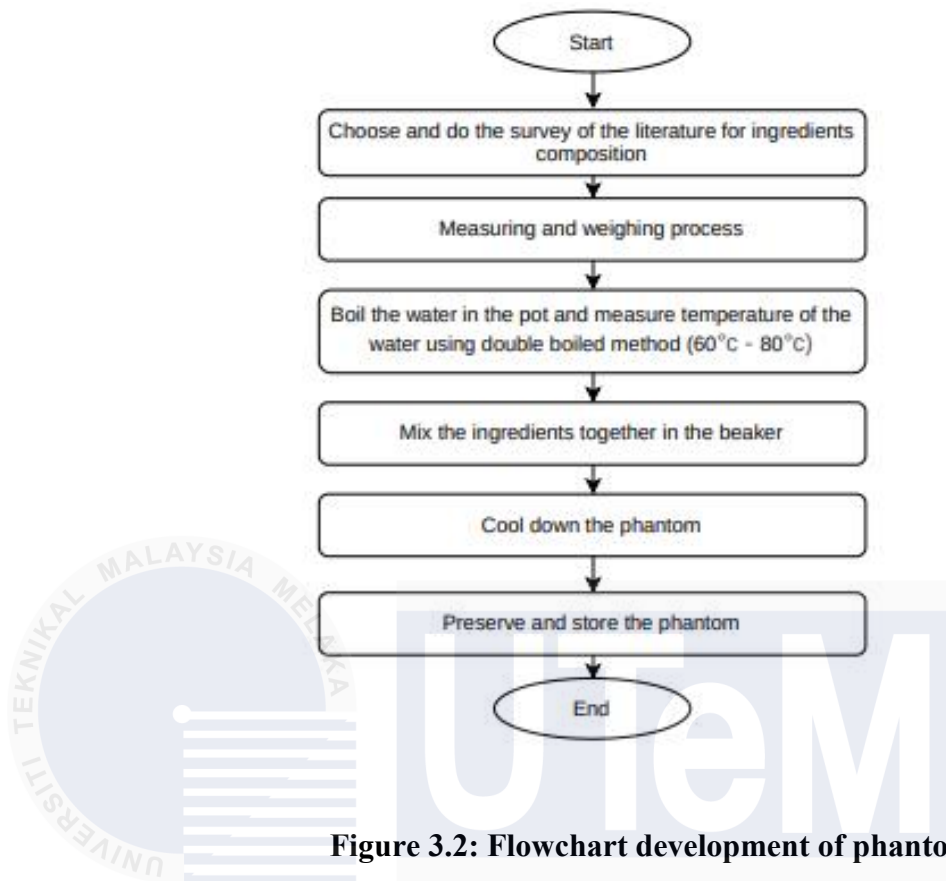


**Figure 3.2: Flowchart development of phantom**

### 3.2.1 Development of Skin Tissue-Equivalent Phantom

Figure 3.3 shows the steps to create the skin tissue-equivalent phantom. Double boiling water ensures even heating and prevents overheating. Maintaining 60°C–80°C water temperature requires a thermometer. Hot water is mixed in a beaker. To mimic human skin's texture and mechanical properties, gradually adding agar and gelatin while stirring creates a gel-like consistency. Xanthan gum and carrageenan powder improve the phantom's stability and elasticity. A thorough stir prevents lumps and ensures uniform distribution. Following titanium dioxide, activated charcoal, silver, graphite, and aluminum powder to mimic human skin, maltodextrin and sodium chloride are carefully added for biochemical simulation. The finished mixture is poured into molds and cooled. Refrigerating the phantom preserves its quality and usefulness for future research.

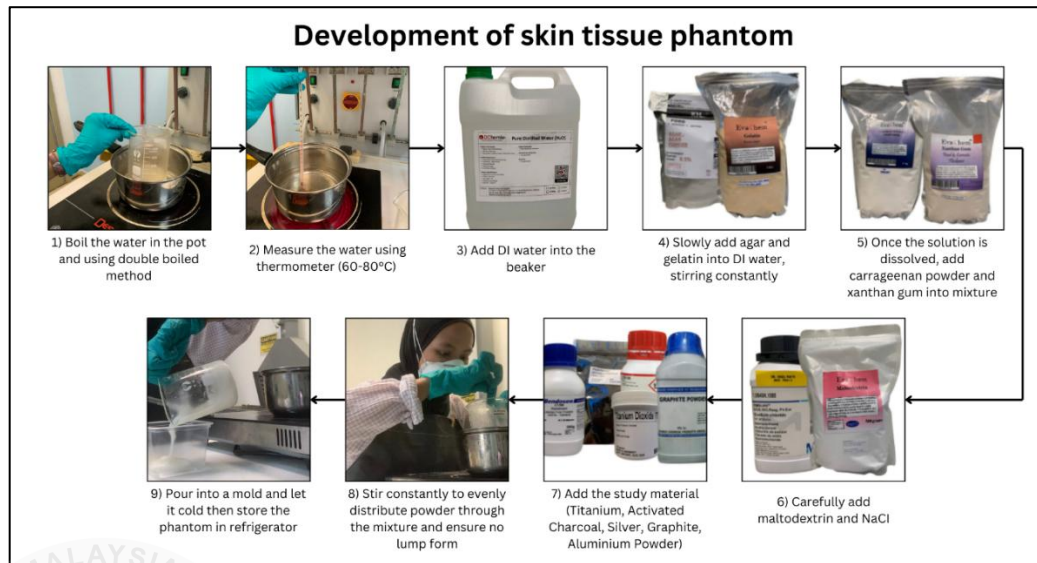


**Figure 3.3: Development of Skin tissue phantom**

### 3.2.2 Development of Fat Tissue-Equivalent Phantom

The fat tissue phantom mimics fat tissue's soft, pliable, slightly heterogeneous texture. According to Figure 3.4, creating the fat tissue-equivalent phantom (F1 - Sample 1) requires several steps. Water is double-boiled and thermometer-monitored to maintain a 60°C–80°C temperature range. Pre-soaking gelatin in deionized water dissolves it completely for smoothness. Glycerin improves texture and flexibility after slowly adding canola oil to mimic fat tissue lipids. Sodium bicarbonate improves isopropanol stability and biochemistry. Corn starch and sodium chloride are slowly stirred into fat tissue to create a slightly heterogeneous texture. Whipping prevents lumps and ensures even distribution. Molds are filled with the prepared solution and cooled to solidify. Finally, the phantom is refrigerated for research or testing to preserve its physical and chemical properties. The product's structure and function match real fat tissue thanks to this precise process.

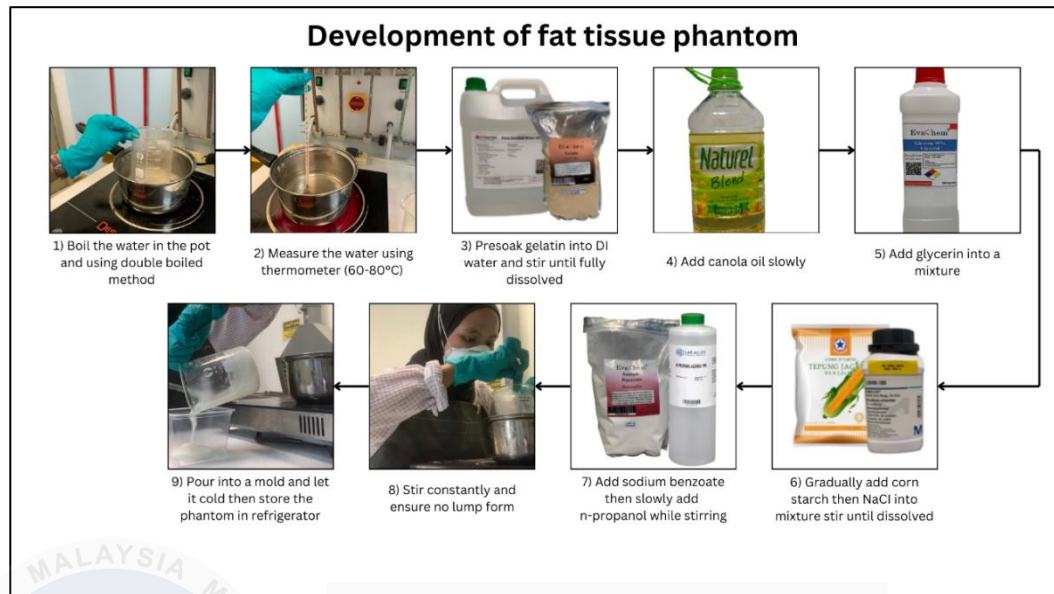


**Figure 3.4: Development of fat tissue phantom (F1 – Sample 1)**

Figure 3.5 also shows how to create the fat tissue-equivalent phantom (F2 - Sample 2), which mimics real fat tissue's texture and properties. To ensure consistent and controlled heating, water is double boiled heated between 60°C and 80°C and monitored with a thermometer. Pre-soaking gelatin in deionized water dissolves and smooths it. To improve structural stability and mimic fat tissue elasticity, xanthan gum and sodium alginate are added. The solution contains sodium chloride (NaCl) and corn starch to mimic fat tissue's biochemical properties and slightly heterogeneous texture. To simulate lipid properties, canola oil is gradually added, followed by silicone emulsion to improve phantom texture and elasticity. For even distribution and lump-free mixing, all ingredients are mixed thoroughly. Pouring the mixture into molds and cooling it in the fridge preserves its structural and chemical properties. For research and testing, this process creates a fat tissue-equivalent phantom that closely resembles real fat tissue.

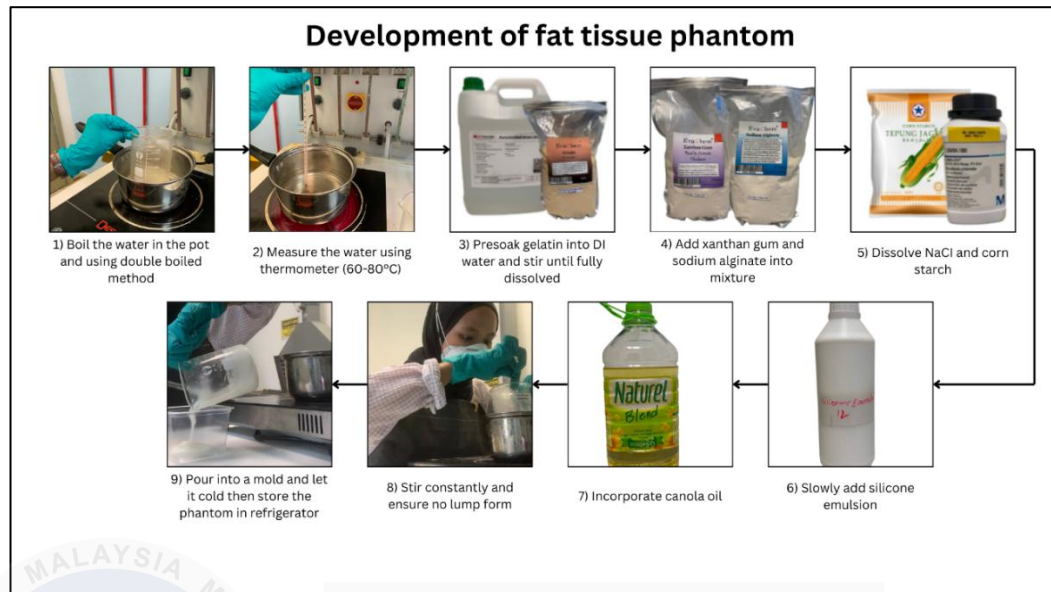


**Figure 3.5: Development of fat tissue phantom (F2 – Sample 2)**

### 3.2.3 Development of Muscle Tissue-Equivalent Phantom

Muscle tissue phantoms are models designed to replicate the physical, mechanical, and optical properties of natural muscle tissue. The development of the muscle tissue-equivalent phantom as shown in Figure 3.6 involves a series of precise steps

to replicate the physical, mechanical, and optical properties of real muscle tissue.

The process begins by boiling water using the double-boil method to maintain consistent heating, with the temperature carefully monitored between 60°C and 80°C.

Gelatin is pre-soaked in deionized water to form a smooth base, followed by the gradual addition of agar, which is stirred continuously to create a stable, gel-like consistency.

Glycerin is then incorporated to enhance elasticity and flexibility, mimicking the properties of muscle tissue. Study materials such as titanium dioxide, activated charcoal, silver, graphite, and aluminum powder are added to replicate the

specific optical and mechanical properties of natural muscle. Maltodextrin and sodium chloride are introduced to improve biochemical and textural characteristics.

The mixture is thoroughly stirred to ensure uniformity, poured into molds, and

The mixture is thoroughly stirred to ensure uniformity, poured into molds, and

allowed to cool, solidifying into the desired shape. Finally, the phantom is stored in a refrigerator to preserve its structural and chemical integrity, ensuring it is ready for research or testing applications.

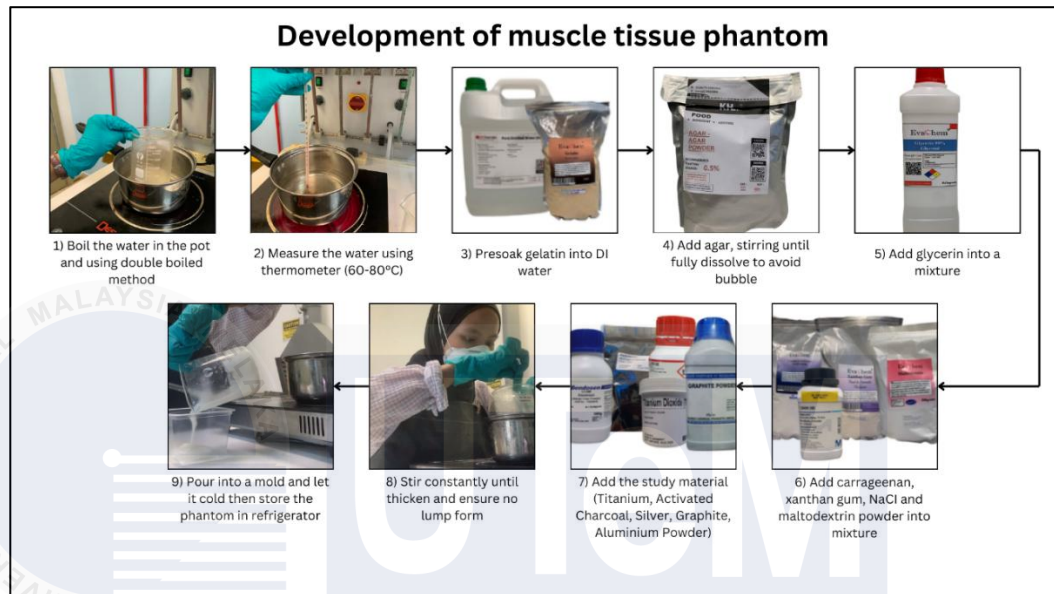


**Figure 3.6: Development of muscle tissue phantom**

### 3.3 Dielectric Properties Measurement

Performing phantom measurements using the E4990A Impedance Analyzer offers a comprehensive approach to characterize the electrical properties of phantoms. The E4990A Impedance Analyzer, with its frequency range of 20 Hz to 120 MHz, provides accurate measurements across a wide range of frequencies, making it suitable for analyzing the low-frequency behavior of phantoms and materials. By combining measurements from this instrument, it can obtain a complete picture of the electrical characteristics of the phantoms over the desired frequency at 1 MHz and 13.56 MHz.



**Figure 3.7: E4990A Impedance Analyzer 20 Hz – 120 MHz**



**Figure 3.8: 16451B Dielectric Test Fixture**

### **3.3.1 16451B Dielectric Test Fixture Calibration**

The Keysight N1500A materials measurement software suite helps accurately determine the electromagnetic properties of various dielectric and magnetic materials. Option 006 for the parallel plate and inductance method is specifically designed for use with E4980A/AL and E4990A instruments [30]. It is compatible with the 16451B and 16452A fixtures, enabling measurement of permittivity, as well as the 16454A fixture for measuring permeability. This option provides a comprehensive solution for accurately determining both permittivity and permeability, essential parameters in various applications such as material characterization and electromagnetic device design.

Calibration must be done sequentially from Step 1 to Step 5 to ensure accuracy. Steps are built on each other to calibrate the system. Missing or rearranging these steps can compromise the calibration process, resulting in inaccurate measurements. Verify that the fixture is set to the correct position according to the calibration method before continuing. Different calibration methods require specific fixture configurations for accurate results. By positioning the fixture properly, it can optimize the calibration process, reducing errors and ensuring accurate measurements.

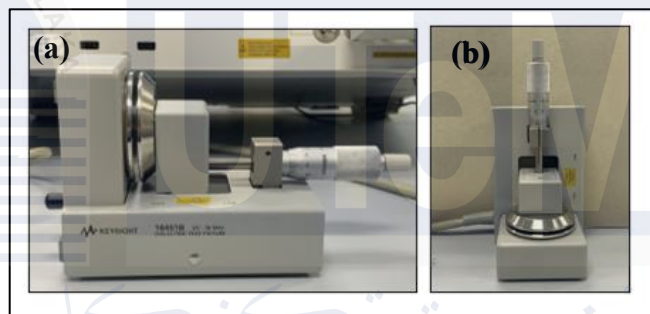


**Figure 3.9: (a) Contact method (vertical position), (b) non-contact method (horizontal position)**

Calibration steps in Table 3.1 show Step 1 through Step 5:

**Table 3.1: Calibration steps for E4990A with 16451B [30]**

Steps	Setup	Explanation
Step 1		<p><u>Adapter Setup – Open</u></p> <ol style="list-style-type: none"> <li>1. Connect 1645B to E4990A.</li> <li>2. Set the 1645B OPEN condition (Attachment WITH cover on MAIN electrode). Then press [OK] to start, [Cancel] to about.</li> </ol>
Step 2		<p><u>Electrode Alignment</u></p> <p>First press [OK] to start. Then</p> <ol style="list-style-type: none"> <li>1. Set the micrometer to 10<math>\mu</math>m.</li> <li>2. Turn the three screws carefully until FAIL disappears. Then press [PASS].</li> </ol>

Step 3		<p><u>Load Compensation</u></p> <p>Then press [OK] to start, then</p> <ol style="list-style-type: none"> <li>1. Set the micrometer to 200<math>\mu</math>m.</li> <li>2. Turn the micrometer's knob slightly until FAIL disappears. Then press [PASS].</li> </ol>
Step 4		<p><u>Open Compensation</u></p> <ol style="list-style-type: none"> <li>1. Set 16451B OPEN condition (Attachment WITH cover on MAIN electrode).</li> <li>2. Then press [OK] to start, [Cancel] to abort.</li> </ol>
Step 5		<p><u>Short Compensation</u></p> <ol style="list-style-type: none"> <li>1. Set 16451B SHORT condition (Attachment WITHOUT cover on COUNTER electrode).</li> <li>2. Then, press [OK] to start, [Cancel] to abort.</li> </ol>

### 3.3.2 Tissue-Equivalent Phantom Measurement setup

Figure 3.11 shows the measurement setup consisting of the test fixture, impedance analyzer and the Tissue-Equivalent phantom as the (MUT).



**Figure 3.10: Measurement setup**

The Keysight 16451B Dielectric Test Fixture is engineered to precisely measure the dielectric constant of solid materials in compliance with ASTM D150 standards. It employs the parallel plate method, positioning the test material between two electrodes to create a capacitor.

It supports dielectric measurements across a frequency range of up to 30 MHz. This broad frequency range allows for accurate analysis of a material's dielectric properties across both low and high-frequency environments. This capability ensures that the fixture can capture a material's behavior accurately across different operating conditions. This equipment can measure parameters of Capacitance (C), Dissipation Factor (D), and Dielectric Constant ( $\epsilon_r'$ ,  $\epsilon_r''$ ).

The test fixture is designed to accept material samples with diameters ranging from 10 mm to 56 mm. This flexibility enables testing of different sample sizes,

from smaller specialized materials to larger dielectric sheets. A consistent and appropriate sample size ensures proper electrode contact and reduces the chances of edge effects or inconsistencies during measurements. In materials testing, the term "*material under testing*" (*MUT*) refers to the sample or specimen being evaluated under specific conditions. In this study, the MUT represents a tissue-equivalent phantom, carefully developed using a mixture of ingredients designed to mimic tissue properties for TET applications.

The analysis of the tissue equivalent phantom's dielectric properties is based on data obtained from Dielectric Test Fixture by using one equipment which is Impedance analyzer. The three terms of dielectric properties permittivity, conductivity and loss tangent of a material can be determined by analyzing its reflection and transmission coefficients.

### 3.3.3 Tissue-Equivalent Phantom Measurement Process

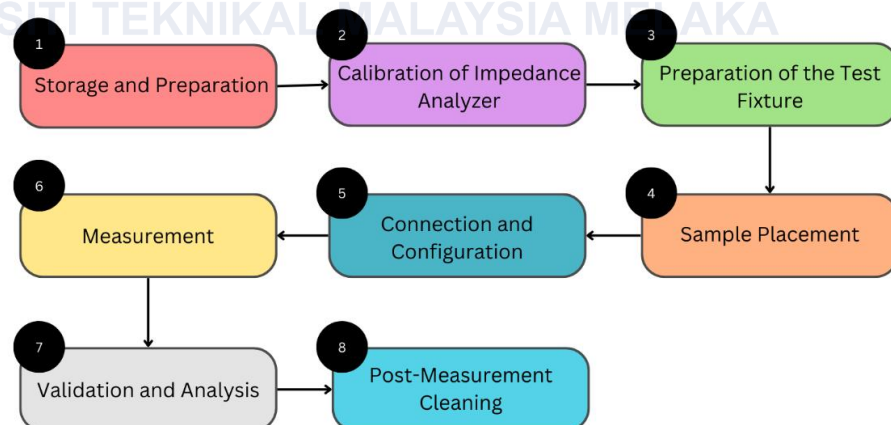


**Figure 3.11: Tissue-Equivalent Phantom Measurement Process**

Figure 3.12 illustrates the tissue-equivalent phantom measurement process:

1. The tissue phantom is stored in a chemical refrigerator to prevent drying and mold growth, ensuring it remains suitable for analysis within a 1-day period to assess its properties.
2. The impedance analyzer is calibrated following manufacturer guidelines to eliminate errors caused by cables, connectors, and test fixtures, ensuring accurate measurements.
3. The test fixture is cleaned, securely connected to the impedance analyzer, and checked for compatibility with the frequency range and material type. The sample is positioned to minimize air gaps and ensure proper electrical contact.
4. The phantom sample is placed in the test fixture.
5. The test fixture is connected to the impedance analyzer using high-quality coaxial cables. The analyzer is configured to the desired frequency range (1 MHz and 13.56 MHz) and voltage level, with measurement settings aligned.
6. A frequency sweep or single-point analysis is conducted to compute dielectric properties including permittivity, conductivity, and loss tangent.
7. Measured values are cross-checked with theoretical or reference tissue properties. The process is repeated for reliability, and data (permittivity, conductivity, loss tangent) is recorded and plotted to assess.
8. The test fixture is thoroughly cleaned to prevent contamination and ensure readiness for future use.

## CHAPTER 4

### RESULTS AND DISCUSSION



This chapter presents the results and analysis of the tissue-equivalent phantom acquired the frequency range of 1 MHz and 13.56 MHz. Tissue-comparable phantom samples were created for each tissue type based on human anatomical parameters, ensuring they closely match the dielectric properties of actual human tissue, including permittivity, conductivity and loss tangent. Each of the samples created is to be compared and focus towards assessing the effect of the tissue-equivalent phantom development with respect to the durability of the phantom. Some data are gathered from IFAC which is an Internet resource for the calculation of the Dielectric Properties of Body Tissues as a reference of three main tissue (SkinWet, Fat and Muscle) at permittivity, loss tangent and conductivity at frequency of 1 MHz and 13.56 MHz. Based on the data collected throughout the semester, the measurements and data collection are kept in an Excel file and plotted into a graph

that to be compared together. Each of the samples is tested up to 1 day after development mimic the tissue phantom by cooking using a double method to study the trend of the graph to ensure the durability and the quality of the tissue phantoms.

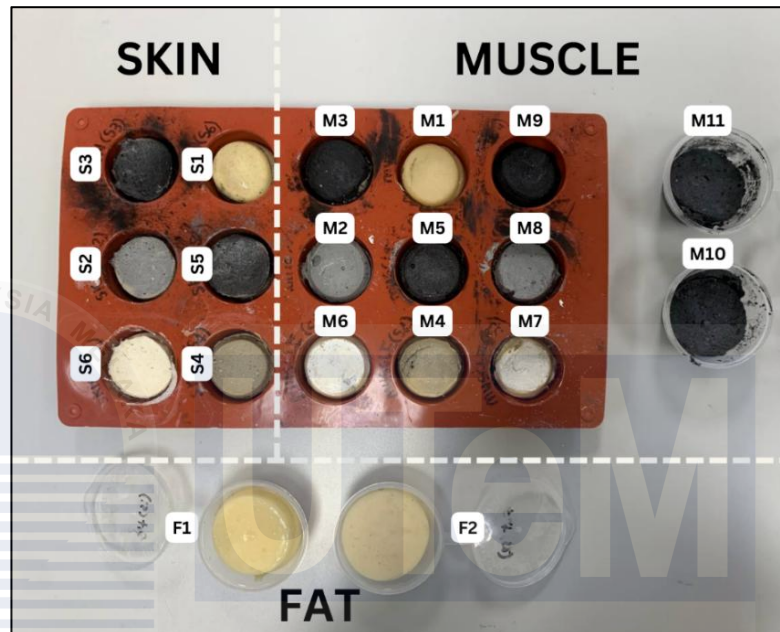


Figure 4.1: Samples of skin, fat and muscle tissue phantom

#### 4.1 Results and analysis of Skin Tissue-Equivalent Phantom

The study focuses on evaluating the dielectric properties of various tissue-equivalent phantom samples to compare them with the dielectric properties of human skin tissue at 1 MHz and 13.56 MHz. Six different phantom samples, including a control sample without any added materials and five others incorporating different conductive or dielectric additives, were prepared for analysis. Each sample has distinct characteristics based on its composition:

- S1 – Sample 1 (Without study material)
- S2 – Sample 2 (Aluminium powder 4%)
- S3 – Sample 3 (Activated charcoal powder 4%)
- S4 – Sample 4 (Silver powder 4%)
- S5 – Sample 5 (Graphite powder 4%)
- S6 – Sample 6 (Titanium Dioxide powder 4%)

#### 4.1.1 Recipe of Skin Tissue-Equivalent Phantom

**Table 4.1: Recipe of Skin Tissue Phantom**

Ingredients (%)	S1	S2	S3	S4	S5	S6
DI Water	58	58	58	58	58	58
Agar	4	4	4	4	4	4
Gelatin	15	15	15	15	15	15
Xanthan gum	2.5	2.5	2.5	2.5	2.5	2.5
Maltodextrin	5.5	5.5	5.5	5.5	5.5	5.5
NaCl	3.5	3.5	3.5	3.5	3.5	3.5
Carrageenan powder	6.5	6.5	6.5	6.5	6.5	6.5
Titanium Dioxide powder	-	-	-	-	-	4
Aluminium powder	-	4	-	-	-	-
Activated Charcoal powder	-	-	4	-	-	-
Silver powder	-	-	-	4	-	-
Graphite powder	-	-	-	-	4	-

#### 4.1.2 Dielectric properties of Skin Tissue-Equivalent Phantom at 1 MHz

Figure 4.2 compares skin tissue-equivalent phantom samples at 1 MHz. The permittivity values for the skin tissue-equivalent phantom samples at 1 MHz reveal notable differences among the samples, reflecting the impact of different study materials. Sample 6, containing 4% titanium dioxide powder, exhibits a permittivity of 1319.47, which is the closest to the reference value of 1832.80, making it the most representative of real tissue properties. Sample 1 (without any study material) and Sample 5 (4% graphite powder) show moderate permittivity values of 1544.68 and 883.60, respectively, aligning partially with the reference. However, extreme values are observed in Sample 3 (4% activated charcoal powder) with the highest permittivity of 2471.42 and Sample 4 (4% silver powder) with the lowest permittivity of 13.67. This indicates that the inclusion of titanium dioxide (Sample 6) provides the most suitable dielectric behavior for skin tissue phantoms, whereas activated charcoal and silver result in significant deviations.

The loss tangent, which measures energy dissipation in the samples, also varies significantly across the six samples. Sample 3, containing 4% activated charcoal powder, has the highest loss tangent of 77.66, indicating excessive energy dissipation compared to the reference value of 15.35. Sample 4, with 4% silver powder, shows the lowest loss tangent of 2.49, suggesting minimal energy dissipation. Among all samples, Sample 6 (titanium dioxide) demonstrates a loss tangent of 2.17, which, although slightly below the reference value, is the most balanced, ensuring a closer representation of the target tissue. The variations in loss tangent highlight that certain study materials, such as activated charcoal and silver, result in less optimal energy dissipation properties, while titanium dioxide offers better alignment.

The conductivity values reflect the samples' ability to conduct electrical current and vary widely across the six samples. Sample 6, containing 4% titanium dioxide, has the highest conductivity of 0.73, which exceeds the reference value of 0.22. This suggests an improved ionic behavior in Sample 6, aligning it closer to real tissue. Samples 1, 2, 3, and 4 exhibit lower conductivity values (ranging from 0.01 to 0.07), indicating reduced ionic flow and less resemblance to the target tissue. Among these, Sample 1 (without study material) and Sample 2 (aluminum powder) show slightly better conductivity compared to others but still fall short of the reference value.

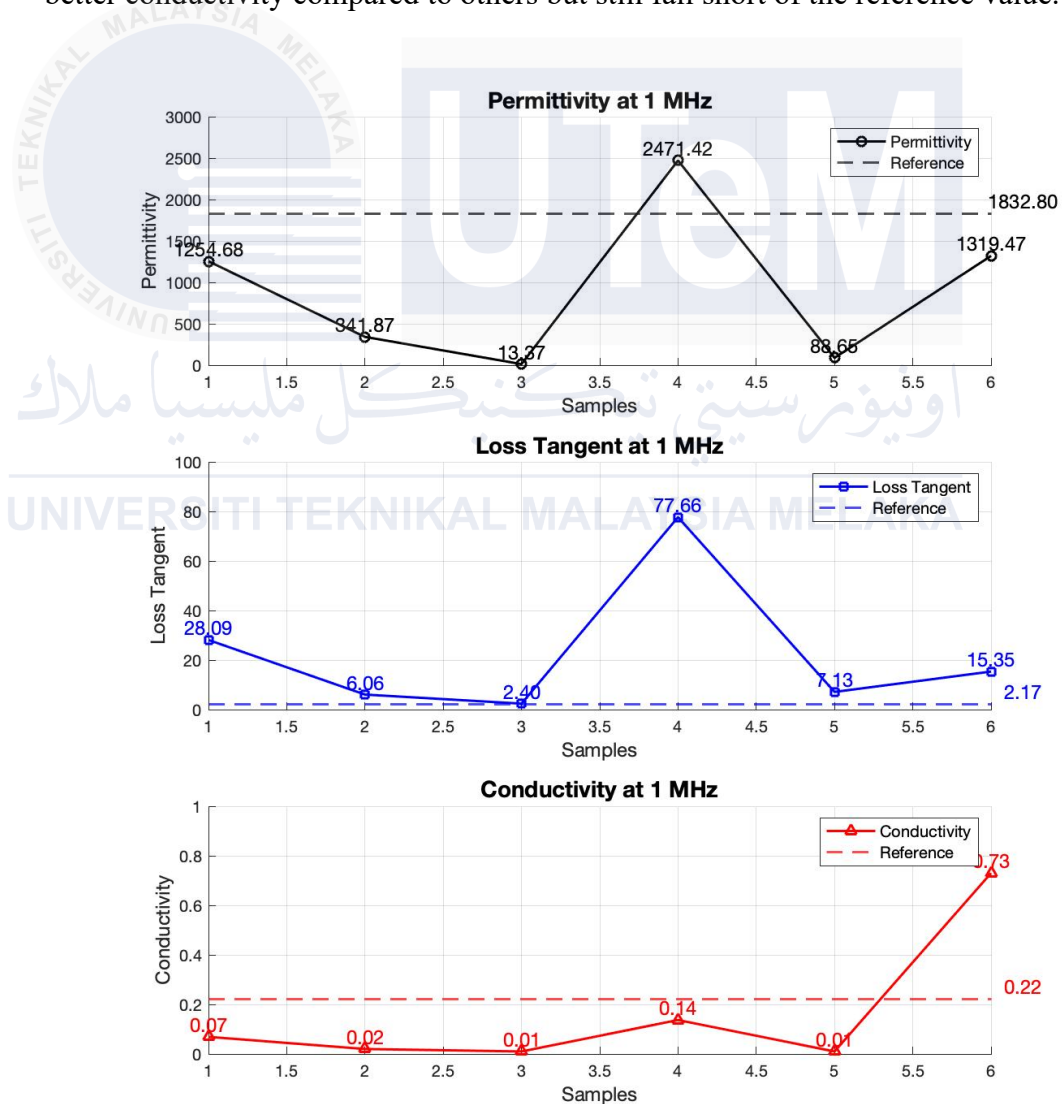


**Figure 4.2: Comparison between permittivity, conductivity and loss tangent for Skin Tissue-Equivalent Phantom Samples at 1 MHz.**

In summary, the analysis of permittivity, loss tangent, and conductivity highlights that Sample 6 which is titanium dioxide powder consistently outperforms the other samples in aligning with the reference dielectric properties of real skin tissue. This suggests that titanium dioxide is the most effective study material for developing skin tissue-equivalent phantoms.

#### 4.1.3 Dielectric properties of Skin Tissue-Equivalent Phantom at 13.56 MHz

Figure 4.3 compares the dielectric properties of skin tissue-equivalent phantom samples at 13.56 MHz. At 13.56 MHz, the permittivity of the skin tissue-equivalent phantom samples exhibits notable variations influenced by the study materials. Sample 3, containing 4% activated charcoal powder, achieves the highest permittivity at 220.90, while Sample 4, with 4% silver powder, records the lowest permittivity at 46.16. The reference permittivity stands at 177.13, serving as the benchmark. Sample 2 (aluminum powder) and Sample 6 (titanium dioxide powder) show permittivity values of 115.15 and 177.13, respectively, with Sample 6 aligning perfectly with the reference value. This makes Sample 6 the most representative of real tissue properties, while the extreme values of Samples 3 and 4 highlight inconsistencies in their dielectric behavior.

The loss tangent, which shows sample energy dissipation, is also variable. Sample 1 (without study material) has the highest loss tangent of 4.14, indicating significant energy dissipation, while Sample 4 (silver powder) has the lowest at 1.35. The reference loss tangent is 2.88. The most balanced energy dissipation sample is Sample 6 (titanium dioxide powder), which matches the reference at 2.88. Samples 1 and 4 differ in their tissue energy loss simulation.

The conductivity results at 13.56 MHz reveal relatively low values for all samples, with slight variations. The reference conductivity is 0.38, while Sample 1 and Sample 4 both achieve the highest value of 0.15. Sample 3 (activated charcoal powder) and Sample 6 (titanium dioxide powder) exhibit the lowest conductivity at 0.01 and 0.08, respectively. Although none of the samples match the reference perfectly, the higher conductivity in Samples 1 and 4 suggests a closer alignment with real tissue properties compared to other samples. However, Sample 6, despite being slightly lower, provides consistent performance across the other properties.

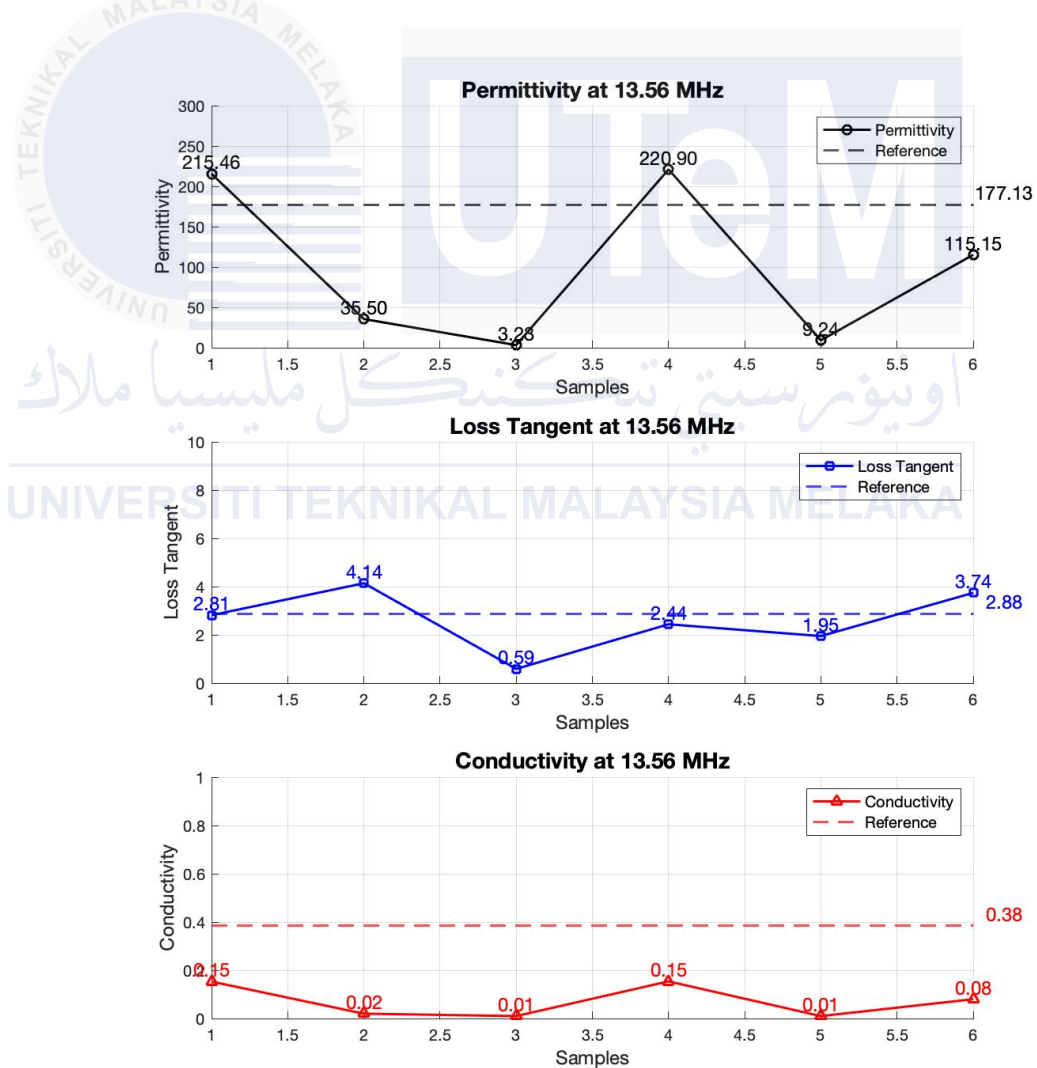


**Figure 4.3: Comparison between permittivity, conductivity and loss tangent for Skin Tissue-Equivalent Phantom Samples at 13.56 MHz.**

At 13.56 MHz, Sample 6 (titanium dioxide powder) emerges as the best-performing phantom, with its permittivity and loss tangent aligning perfectly with the reference values. Overall, Sample 6 demonstrates superior consistency and accuracy in representing the dielectric properties of skin tissue.

## 4.2 Results and analysis of Fat Tissue-Equivalent Phantom

The study focuses on evaluating the dielectric properties of various tissue-equivalent phantom samples to compare them with the dielectric properties of human fat tissue at 1 MHz and 13.56 MHz. Two different phantom samples, including a control sample, were prepared for analysis. Each sample has distinct characteristics based on its composition:

- F1 – Sample 1
- F2 – Sample 2

### 4.2.1 Recipe of Fat Tissue-Equivalent Phantom

**Table 4.2: Recipe of Fat Tissue Phantom**

Ingredients (%)	F1	F2
Canola oil	25.8	25.8
Glycerin	15	-
DI Water	16	16
Gelatin	12	12
N-Propanol	10	-
Corn Starch	20	20.6
Sodium Benzoate	0.6	-
NaCl	0.6	0.6
Xanthan gum	-	8
Silicone Emulsion	-	15
Sodium Alginate powder	-	2

#### 4.2.2 Dielectric properties of Fat Tissue-Equivalent phantom at 1 MHz and 13.56 MHz

Dielectric properties of fat tissue-equivalent phantom samples at 1 MHz and 13.56 MHz are shown in Figure 4.4. Sample 1 and Sample 2 have different permittivity at 1 MHz and 13.56 MHz for fat tissue-equivalent phantoms. Sample 1 has a high permittivity of 230.39 at 1 MHz, closer to the reference value of 239.01, which matches fat tissue properties. Sample 2 has a 56.67 permittivity, indicating less electrical energy storage. Both samples' permittivity decreases at 13.56 MHz, with Sample 1 at 27.32 and Sample 2 at 16.83, showing similar trends but still deviating significantly from the reference value. Sample 1 is more representative of fat tissue because it is closer to the reference at both frequencies.

The loss tangent, which measures material energy dissipation, varies greatly across frequencies and samples. Sample 1's loss tangent at 1 MHz is 18.66, closer to the reference value of 13.66, while Sample 2's is 99.30, indicating excessive energy dissipation. Both samples have reduced loss tangents at 13.56 MHz, Sample 1 at 3.40 and Sample 2 at 18.56. Sample 2 loses more energy than Sample 1, but its performance improves at higher frequencies. Sample 1's lower loss tangent makes it better for fat tissue modeling.

The two samples' and frequencies' conductivity vary greatly. Sample 1's conductivity at 1 MHz is 0.01, matching the reference value, while Sample 2's is 0.02. Both samples increase conductivity at 13.56 MHz, Sample 1 at 0.03 and Sample 2 at 0.04. Sample 1's conductivity is closer to the reference value at both frequencies despite the increase, better representing fat tissue electrical behavior.

Comparison of Fat Tissue-Equivalent Phantom Samples at 1 MHz and 13.56 MHz

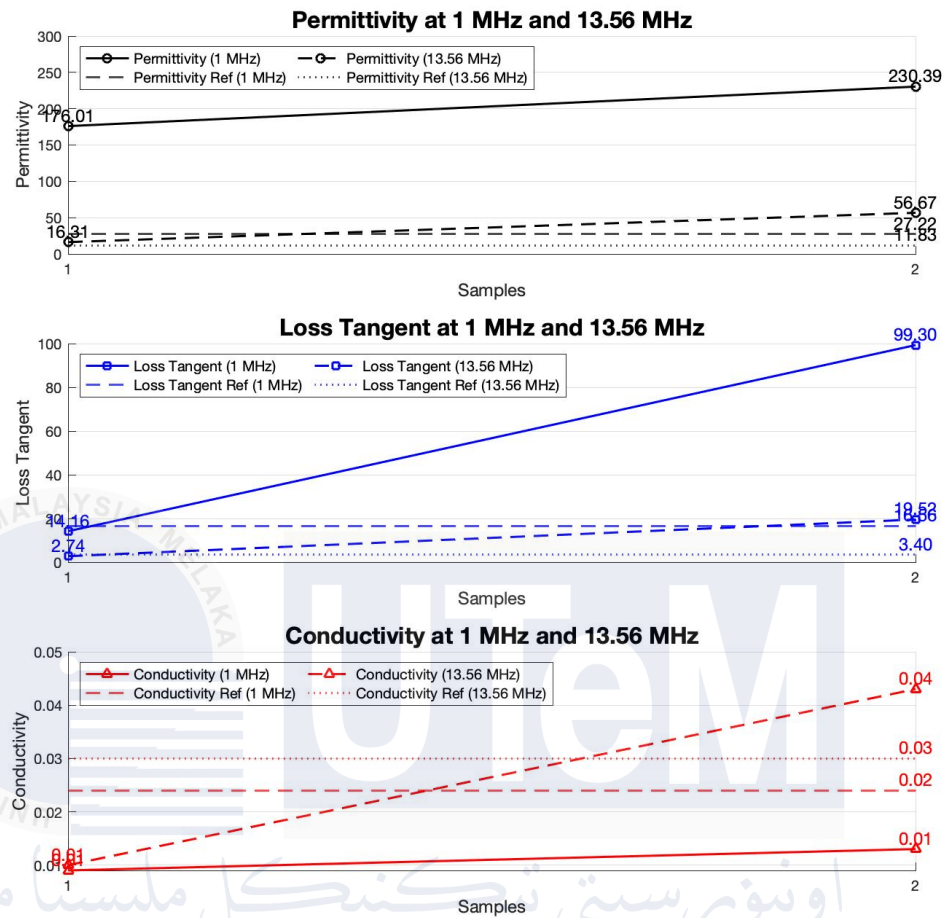


**Figure 4.4: Comparison between permittivity, conductivity and loss tangent for Fat Tissue-Equivalent Phantom Samples at 1 MHz and 13.56 MHz.**

In Summary, Sample 1 outperforms Sample 2 in all three dielectric properties at 1 MHz and 13.56 MHz. Its permittivity, loss tangent, and conductivity values match reference values better, mimicking fat tissue properties. Sample 2 improves loss tangent at higher frequencies but deviates significantly in permittivity and conductivity, making it unsuitable for fat tissue equivalence applications. Fat tissue-equivalent phantoms are best made from Sample 1.

### 4.3 Results and Analysis of Tissue-Equivalent Phantom

The study compares tissue-equivalent phantom dielectric properties to human muscle tissue at 1 MHz and 13.56 MHz. Phantom samples were prepared for analysis, including a control sample without additives and ten with different permittivity, conductivity, and loss tangent. The composition of each sample determines its characteristics:

- M1 – Sample 1 (Without study material)
- M2 – Sample 2 (Aluminium powder 4%)
- M3 – Sample 3 (Activated charcoal powder 4%)
- M4 – Sample 4 (Silver powder 4%)
- M5 – Sample 5 (Graphite powder 4%)
- M6 – Sample 6 (Titanium Dioxide powder 4%)
- M7 – Sample 7 (Aluminium powder 8%)
- M8 – Sample 8 (Activated charcoal powder 8%)
- M9 – Sample 9 (Silver powder 8%)
- M10 – Sample 10 (Graphite powder 8%)
- M11 – Sample 11 (Titanium Dioxide powder 8%)

#### 4.3.1 Recipe for Muscle Tissue-Equivalent Phantom

Table 4.3 shows the ingredient recipe of mimic the muscle tissue phantom. The research aims to analyze the evaluation of these properties that focus on the field to focus towards assessing the effect of the tissue equivalent phantom development with respect to the durability of the phantom by comparing results data of the dielectric properties in terms of permittivity, loss tangent and conductivity. This comparative method will enable a gradual evaluation of the developed phantoms,

leading to the identification of the most suitable dielectric properties for the skin tissue phantom.

**Table 4.3: Recipe of Muscle Tissue Phantom**

Ingredients (%)	M1	M2	M3	M4	M5	M6	M7	M8	M9	M10	M11
DI Water	55	55	55	55	55	55	55	55	55	55	55
Agar	5	5	5	5	5	5	4	4	4	4	4
Gelatin	16	16	16	16	16	16	15	15	15	15	15
Xanthan gum	3.4	3.4	3.4	3.4	3.4	3.4	2.4	2.4	2.4	2.4	2.4
Maltodextrin	6	6	6	6	6	6	5	5	5	5	5
NaCl	1.8	1.8	1.8	1.8	1.8	1.8	1.8	1.8	1.8	1.8	1.8
Glycerin	2.8	2.8	2.8	2.8	2.8	2.8	1.8	1.8	1.8	1.8	1.8
Carrageenan powder	5	5	5	5	5	5	5	5	5	5	5
Titanium Dioxide powder	-	-	-	-	-	4	8	-	-	-	-
Aluminium powder	-	4	-	-	-	-	-	8	-	-	-
Activated Charcoal powder	-	-	4	-	-	-	-	-	8	-	-
Silver powder	-	-	-	4	-	-	-	-	-	8	-
Graphite powder	-	-	-	-	4	-	-	-	-	-	8

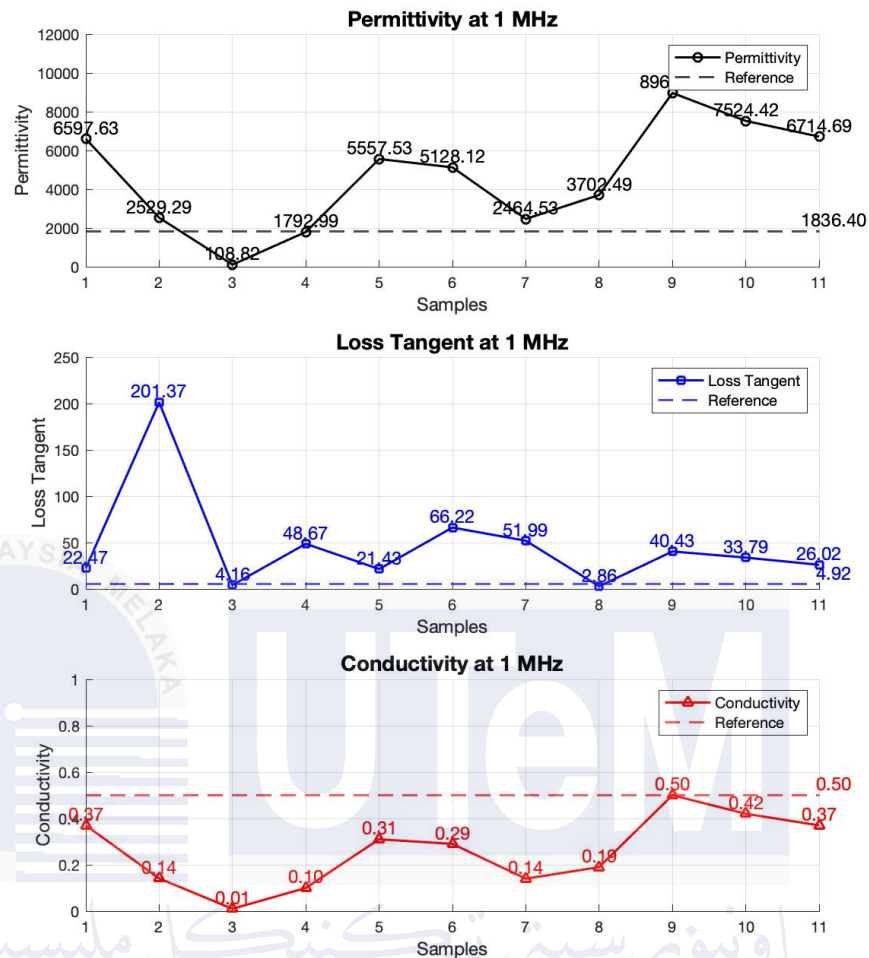
#### 4.3.2 Dielectric properties of Muscle Tissue Phantom at 1MHz

Figure 4.5 compares the dielectric properties of muscle tissue-equivalent phantom samples at 1 MHz. At 1 MHz, the permittivity of muscle tissue-equivalent phantom samples varies widely, with Sample M4 (Silver powder, 4%) emerging as the best-performing sample. M4 achieves a permittivity value of 1792.99, which is closest to the reference value of 1836.40, indicating its strong ability to replicate the dielectric storage properties of real muscle tissue. In contrast, Sample M9 (Activated charcoal powder, 8%) has the highest permittivity at 8968.21, and Sample M3 (Activated

charcoal powder, 4%) records the lowest at 108.82, both deviating significantly from the reference. This highlights that while higher concentrations of silver increase permittivity, the 4% concentration in M4 achieves the most balanced and realistic value, making it the best choice for permittivity among the samples.

The loss tangent values, representing energy dissipation, show considerable variation across the samples. Sample M2 (Aluminum powder, 4%) records the highest loss tangent at 201.37, indicating excessive energy loss, while Sample M8 (Activated charcoal powder, 8%) has the lowest value at 2.86, showing minimal dissipation. The reference value of 22.47 serves as a benchmark, and most samples deviate significantly. While Sample M4 performs well in permittivity, its loss tangent of 21.43 is relatively close to the reference value, indicating it also balances energy dissipation well compared to other samples. Samples M10 (Graphite powder, 8%) and M11 (Titanium dioxide powder, 8%) also perform moderately in terms of loss tangent.

Conductivity, reflecting the sample's ability to conduct electrical current, also varies across the materials. The reference value is 0.50, with Samples M8 (Activated charcoal powder, 8%) and M9 (Silver powder, 8%) matching the reference perfectly, indicating excellent conductivity. Conversely, Sample M3 (Activated charcoal powder, 4%) and Sample M4 (Silver powder, 4%) record the lowest conductivity at 0.01 and 0.10, respectively. Despite its lower conductivity, Sample M4 compensates with its superior permittivity performance, making it a strong candidate for applications prioritizing dielectric storage over conductivity.



**Figure 4.5: Comparison between permittivity, conductivity and loss tangent for Muscle Tissue-Equivalent Phantom Samples at 1 MHz**

In summary, while permittivity is the focus then Sample M4 (Silver powder, 4%) emerges as the best-performing sample, closely aligning with the reference value and achieving a balanced performance.

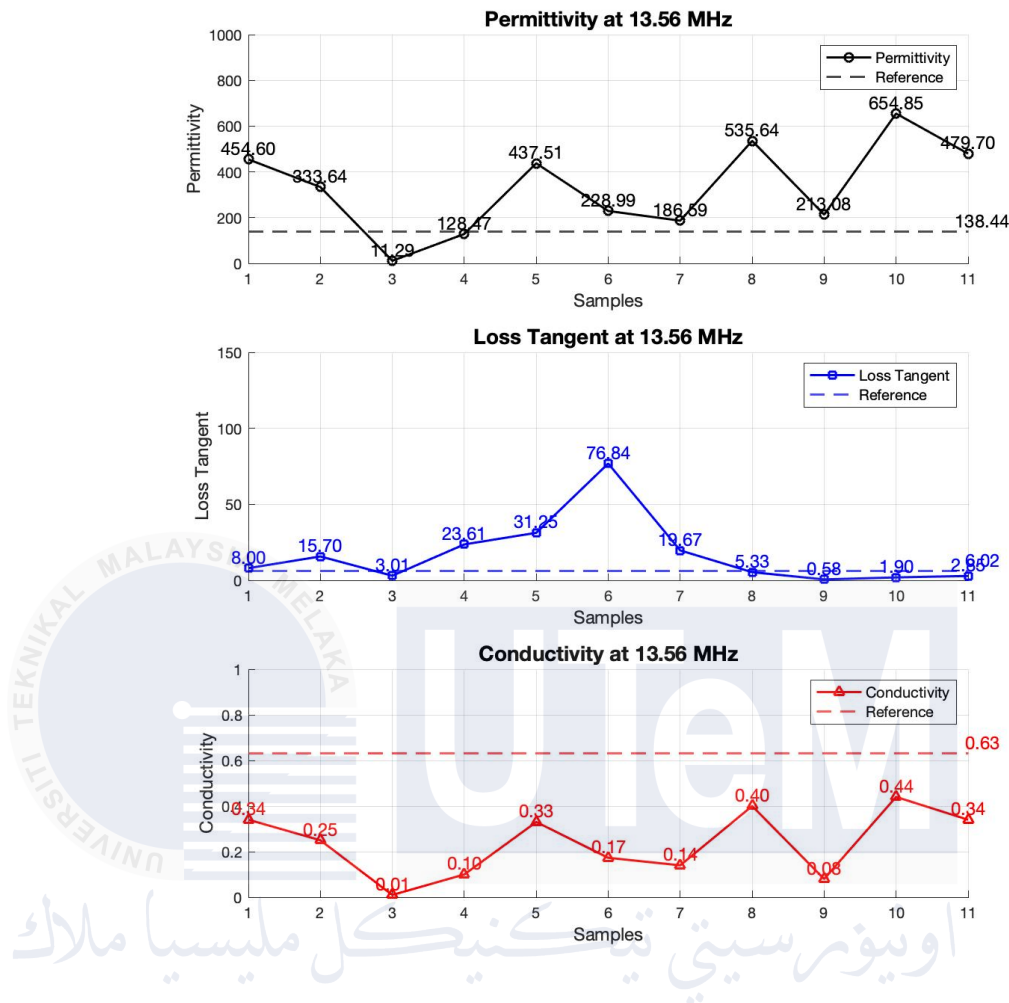
### 4.3.3 Dielectric properties of Muscle Tissue Phantom at 13.56 MHz

Figure 4.6 shows comparing the permittivity of tissue-equivalent phantom samples with human muscle tissue at 13.56 MHz. At 13.56 MHz, the best-performing sample in terms of permittivity is M4 (Silver powder, 4%), with a value of 138.64, which is closest to the reference value of 138.44. This alignment indicates that Sample M4 effectively replicates the dielectric storage properties of real muscle

tissue. In contrast, other samples, such as M9 (Silver powder, 8%) with a high permittivity of 654.85, and M3 (Activated charcoal powder, 4%) with a low value of 128.47, deviate significantly from the reference. These results highlight that silver powder at a 4% concentration achieves the most balanced and realistic permittivity, making M4 the optimal choice for this parameter.

The loss tangent values, which measure energy dissipation, vary widely among the samples. Sample M6 (Titanium dioxide powder, 4%) exhibits the highest loss tangent at 76.84, reflecting excessive energy loss. On the other hand, Sample M8 (Activated charcoal powder, 8%) achieves the lowest value at 2.86, which is nearly identical to the reference value of 2.60. Sample M4 (Silver powder, 4%) also performs well in this category, with a loss tangent of 3.01, aligning closely with reference. This indicates that M4 not only excels in permittivity but also maintains energy dissipation close to the target range, further supporting its suitability.

In terms of conductivity, the reference value is 0.63, and Sample M9 (Silver powder, 8%) perfectly matches this benchmark, demonstrating excellent electrical conductivity. Sample M8 (Activated charcoal powder, 8%) also performs well, with a conductivity of 0.44, indicating good ionic movement. Conversely, Sample M4 records a relatively low conductivity of 0.01, which is its weakest point. Despite this limitation, the exceptional performance of Sample M4 in permittivity and loss tangent compensates for its lower conductivity, depending on the intended application.



**Figure 4.6: Comparison between permittivity, conductivity and loss tangent for Muscle Tissue-Equivalent Phantom Samples at 13.56 MHz**

In summary, at 13.56 MHz that Sample M4 (Silver powder, 4%) emerges as the best-performing sample for permittivity, aligning almost perfectly with the reference value. Additionally, it demonstrates good performance in loss tangent, further solidifying its position as the most representative sample for muscle tissue properties. While its conductivity is lower than ideal, its superiority in dielectric storage and energy dissipation makes it the optimal choice for applications where permittivity is the primary focus.

#### 4.4 Effect of ingredients with the Tissues-Equivalent phantom

Table 4.4: The study material 4% effect in skin tissue phantom (Permittivity)

Samples (4%)		Frequency (Hz)	
		1 MHz	13.56 MHz
		Permittivity of Human Skin Tissue References 1 MHz: 1832.8	Permittivity of Human Skin Tissue References 13.56 MHz: 177.13
Aluminium powder	S2	341.84	35.50
Activated Charcoal powder	S3	13.37	3.23
Silver powder	S4	2471.42	220.896
Graphite powder	S5	88.65	9.23
Titanium dioxide (TiO <sub>2</sub> ) powder	S6	1319.47	115.15

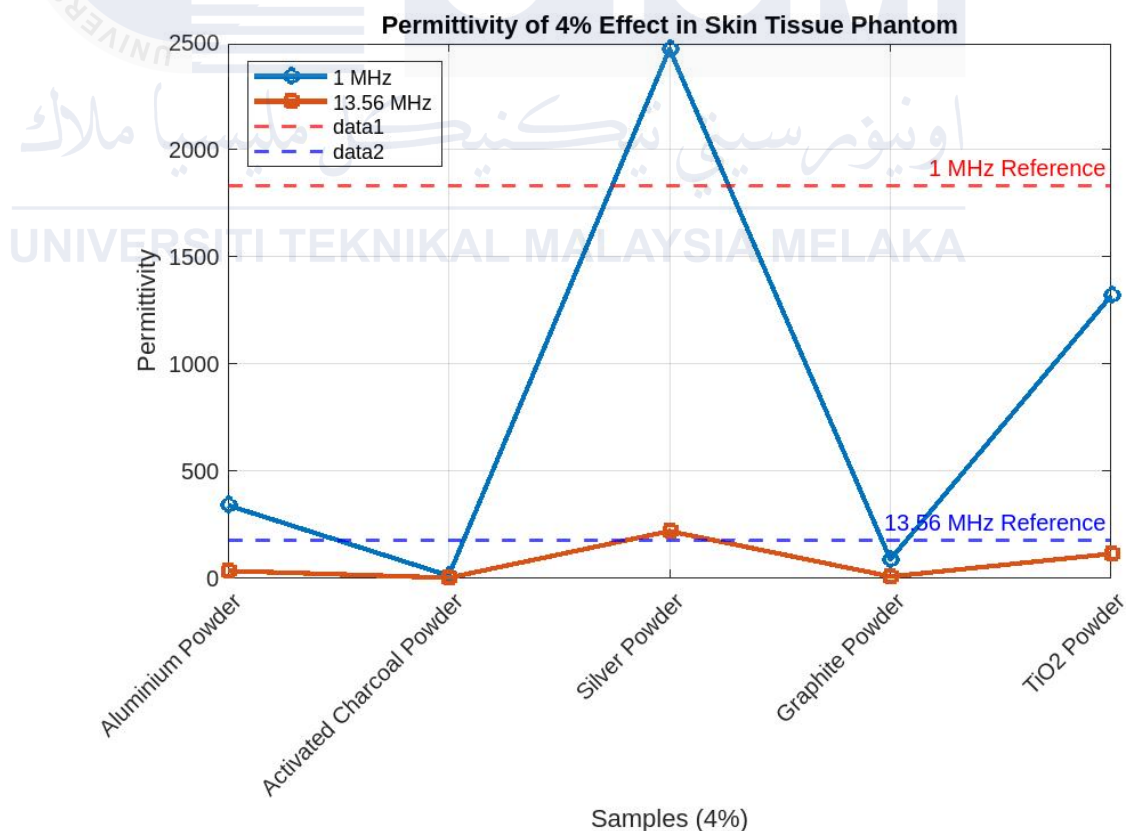


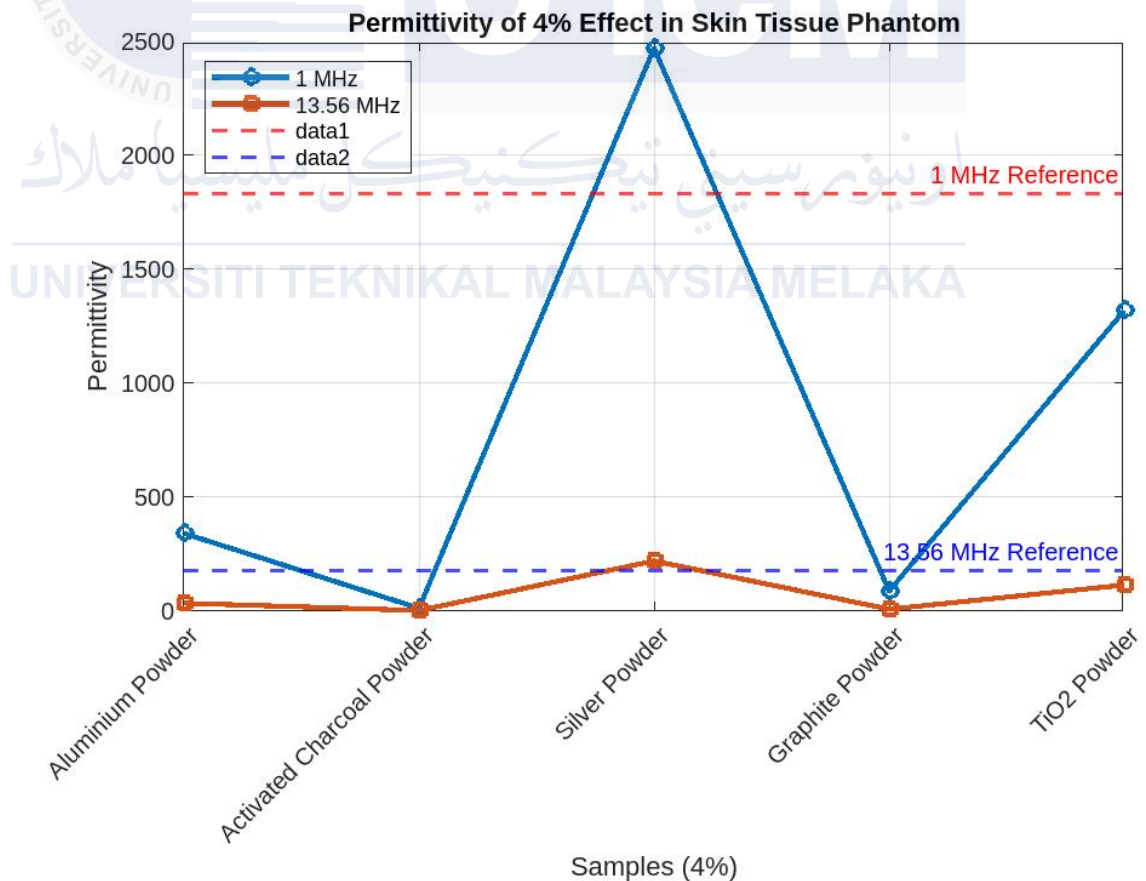
Figure 4.7: Permittivity of 4% effect in Skin Tissue Phantom

Table 4.4 and Figure 4.7 show the study investigates the effect of 4% study materials on the permittivity of skin tissue phantom at 1 MHz and 13.56 MHz, compared to human skin tissue references (1832.8 at 1 MHz and 177.13 at 13.56 MHz). Among the materials, Titanium dioxide ( $\text{TiO}_2$ ) powder (S6) demonstrates the best compatibility with human skin tissue, showing permittivity values of 1319.47 at 1 MHz and 115.15 at 13.56 MHz, which are closer to the reference compared to other samples. Silver powder (S4) exhibits excessive permittivity at 1 MHz (2471.42) but is relatively closer at 13.56 MHz (220.896). Graphite powder (S5) and Aluminium powder (S2) show significantly lower permittivity values at both frequencies, with values like 88.65 and 341.84 at 1 MHz, respectively, making them less suitable. Activated Charcoal Powder (S3) has the lowest permittivity among all materials at both frequencies (13.37 at 1 MHz and 3.23 at 13.56 MHz), demonstrating poor alignment with human skin tissue properties.

Overall, Titanium dioxide ( $\text{TiO}_2$ ) powder (S6) is identified as the most suitable material for skin tissue phantom replication. Titanium dioxide ( $\text{TiO}_2$ ) powder is commonly used in developing tissue-equivalent phantoms due to its effective light-scattering properties, which help simulate the optical characteristics of biological tissues. For instance, a study published in the Journal of Biomedical Optics discusses the use of  $\text{TiO}_2$  powder in creating 3D-printed tissue-simulating phantoms for near-infrared fluorescence imaging, highlighting its role in mimicking tissue optical properties [31]. Additionally, research on multimodal liver phantoms has utilized  $\text{TiO}_2$  as a scattering agent to replicate the optical and acoustic properties of liver tissue, demonstrating its versatility in phantom development [32].

**Table 4.5: The study material 4% effect in muscle tissue phantom (Permittivity)**

Samples (4%)		1 MHz Permittivity of Human Muscle Tissue References 1 MHz: 1836.4	13.56 MHz Permittivity of Human Muscle Tissue References 13.56 MHz: 138.44
Aluminium powder	M2	341.84	35.50
Activated Charcoal powder	M3	13.37	3.23
Silver powder	M4	2471.42	220.896
Graphite powder	M5	88.65	9.23
Titanium dioxide (TiO <sub>2</sub> ) powder	M6	1319.47	115.15



**Figure 4.8: Permittivity of 4% effect in Muscle Tissue Phantom**

**Table 4.6: The study material 8% effect in muscle tissue phantom (Permittivity)**

Samples (8%)		Frequency (Hz)	
		1 MHz	13.56 MHz
		Permittivity of Human Muscle Tissue References 1 MHz: 1836.4	Permittivity of Human Muscle Tissue References 13.56 MHz: 138.44
Titanium dioxide (TiO <sub>2</sub> ) powder	M7	2464.53	186.60
Aluminium powder	M8	3702.49	535.64
Activated Charcoal powder	M9	8968.21	213.08
Silver powder	M10	7524.42	654.85
Graphite powder	M11	6714.69	479.70

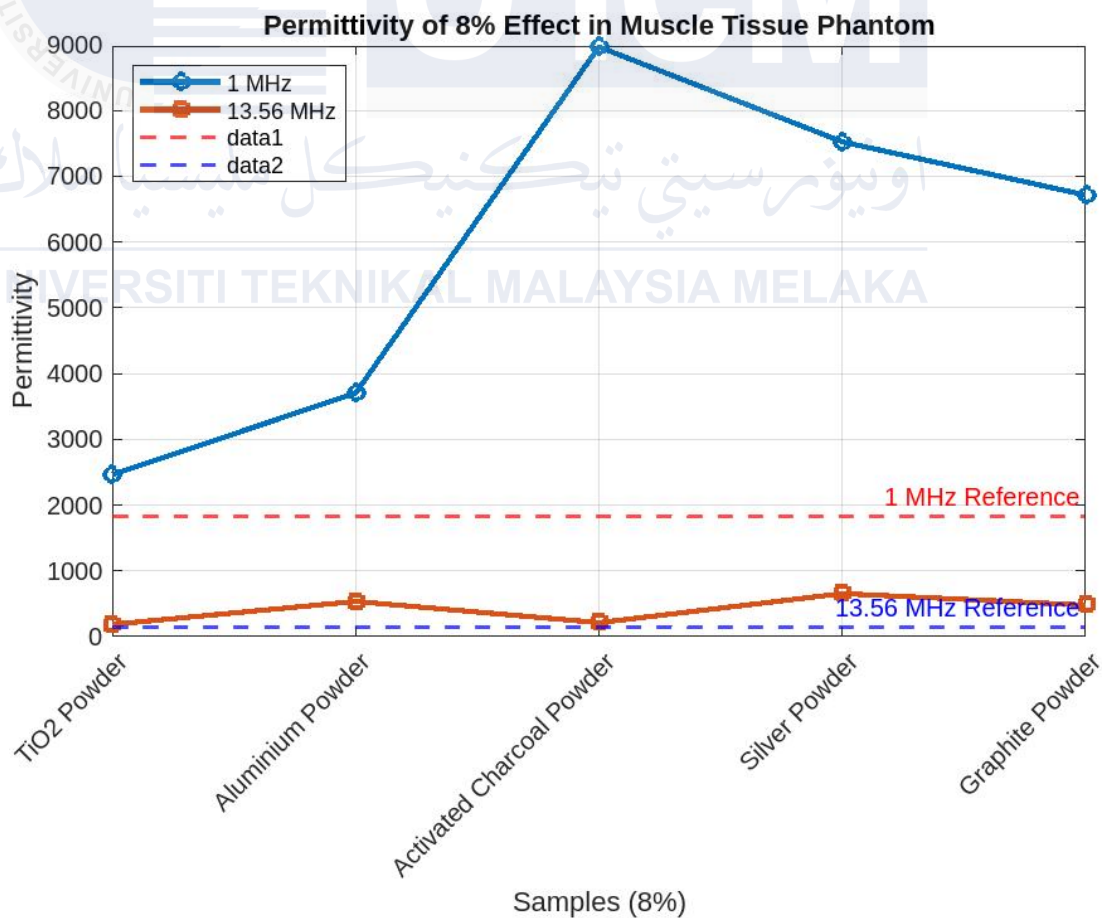


**Figure 4.9: Permittivity of 8% effect in muscle tissue phantom**

Tables (4.5 and 4.6) and Figure (4.8 and 4.9) compare the effects of 4% and 8% study materials on the permittivity of muscle tissue phantom at 1 MHz and 13.56 MHz, with human muscle tissue references of 1836.4 (1 MHz) and 138.44 (13.56 MHz). For 4% samples, Titanium dioxide ( $\text{TiO}_2$ ) powder (M6) shows the best alignment, with permittivity values of 1319.47 at 1 MHz and 115.15 at 13.56 MHz, closer to the references than other materials. Silver powder (M4) exceeds the references significantly, with 2471.42 at 1 MHz and 220.896 at 13.56 MHz. Other materials, such as Aluminium powder (M2), Graphite powder (M5), and Activated Charcoal powder (M3), display much lower permittivity values, making them less suitable for muscle tissue replication.

For 8% samples, permittivity values increase significantly across all materials. Titanium dioxide ( $\text{TiO}_2$ ) powder (M7) demonstrates moderate alignment, with 2464.53 at 1 MHz and 186.60 at 13.56 MHz, closer to the references compared to other materials. Activated Charcoal powder (M9) and Graphite powder (M11) exhibit extremely high values at both frequencies, such as 8968.21 and 6714.69 at 1 MHz, making them unsuitable. Silver powder (M10) and Aluminium powder (M8) also show excessive values, particularly at 13.56 MHz (654.85 and 535.64, respectively).

The 4% samples, particularly Titanium dioxide ( $\text{TiO}_2$ ) powder (M6), provide better compatibility with human muscle tissue references than the 8% samples, which show exaggerated permittivity values, reducing their suitability for muscle tissue phantom replication.

#### 4.5 Validation Tissue-Equivalent Phantom by using the Transcutaneous Transfer Energy (TET) Application for 1 MHz

A Transcutaneous Energy Transfer (TET) application validates a tissue-equivalent phantom by selecting materials that mimic human tissue's electrical properties, such as water, gels, or polymers. After preparation and calibration, the phantom is exposed to an energy transfer system, which may use inductive or capacitive coupling, to simulate human tissue during energy transfer testing.

A tissue-equivalent phantom is validated with the TET system by seeing if it reacts to energy like human tissue. A phantom made from skin, fat, and muscle-like materials is tested for energy absorption using energy transfer systems. The phantom's power loss, temperature, and electric fields are measured to ensure tissue mimicry. If it acts like human tissue, it can be used for further testing to ensure the Transcutaneous Energy Transfer (TET) application system works in medical devices.

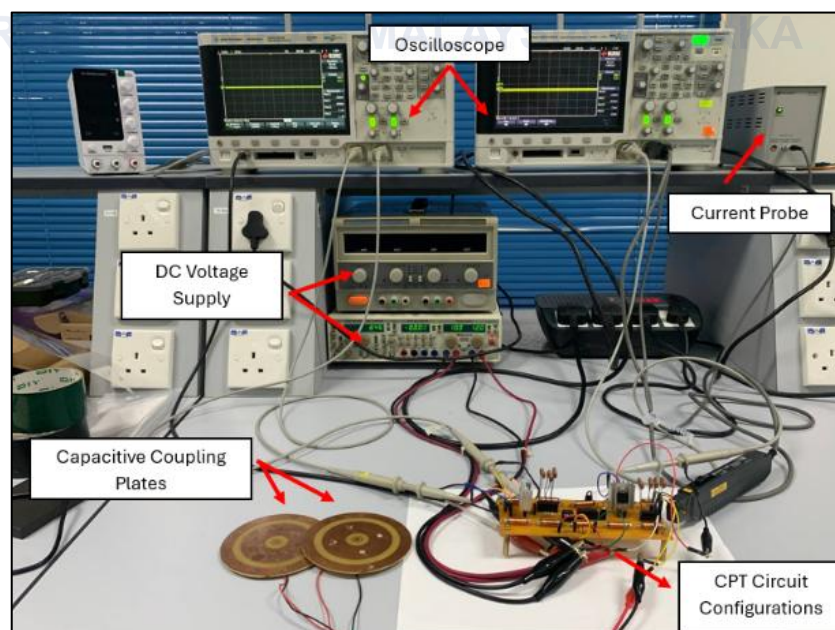
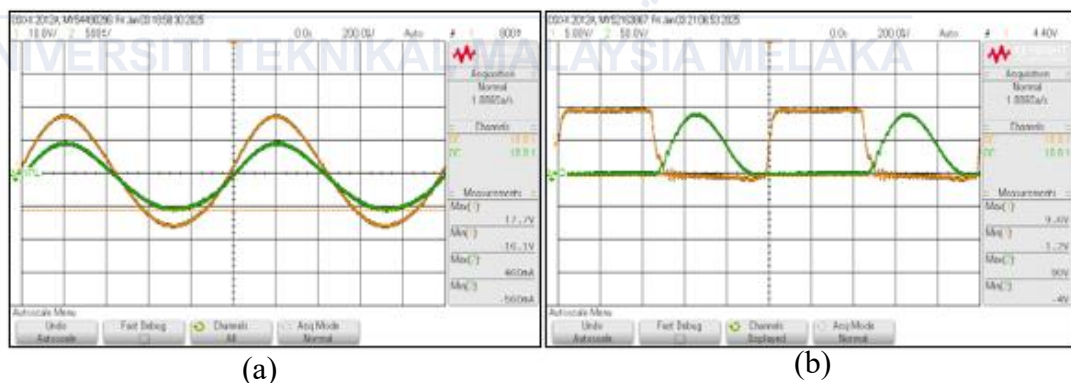


Figure 4.10: TET Setup

The setup in Figure 4.10 shown demonstrates a Transcutaneous Energy Transfer (TET) system operating at a frequency of 1 MHz, which is suitable for efficient wireless energy transfer in applications such as medical implants and wearable devices. The DC voltage supply provides a stable input that powers the system, which is then converted into a high-frequency AC signal by the CPT (Capacitive Power Transfer) circuit. The capacitive coupling plates serve as the medium for energy transfer by creating an alternating electric field at the 1 MHz frequency, enabling non-contact power delivery. An oscilloscope monitors critical voltage and current waveforms at this frequency to evaluate the system's efficiency, while a current probe measures the real-time current to ensure proper operation and energy transfer performance. The 1 MHz frequency is chosen to optimize the balance between energy transfer efficiency and minimizing losses, making the setup ideal for experimental analysis of wireless power transfer systems in practical applications.



**Figure 4.11: (a) IV original and (b) ZVS original**

The validation phantom for TET applications at 1 MHz demonstrates the effectiveness of the Class-E resonant inverter circuit for wireless energy transfer. The circuit, tuned for resonance at 1 MHz, achieves Zero Voltage Switching (ZVS), as shown by the waveforms, ensuring minimal switching losses and high efficiency.

TET technology, crucial for biomedical implants, benefits from the high frequency, which enables efficient energy transfer with minimal tissue heating. The validation setup mimicking human tissue confirms the system's ability to transfer power effectively and safely, showcasing its potential for real-world applications in biomedical and other high-frequency systems. This validation not only confirms the theoretical design but also proves its capability in practical scenarios, making it a valuable contribution to the development of wireless energy transfer systems for biomedical and other high-frequency applications.

#### **4.5.1 The Validation Process of Skin, Fat and Muscle Tissue-Equivalent Phantom**

Validating skin, fat, and muscle phantoms is crucial to ensure they accurately replicate the physical, optical, and mechanical properties of real human tissues. The validation process typically involves several key steps, including material characterization, property measurement, and performance testing in relevant applications.

#### **4.5.2 The Validation process of Skin Tissue-Equivalent Phantom**

The skin tissue phantom's dielectric properties and energy transfer efficiency when interfaced with skin-like material are tested during validation. Figure 4.12 shows that the skin tissue phantom mimics the electrical and physical properties of real human skin to ensure efficient power transfer and TET performance. As shown in Figure 4.13(a), the circuit's current-voltage (IV) characteristics with the skin phantom are then analyzed. This analysis assesses energy transfer efficiency and circuit stability under simulated skin conditions. Finally, Figure 4.13(b) shows Zero Voltage Switching (ZVS), where the MOSFET voltage drops to zero before

switching. This reduces switching losses, making the circuit efficient and suitable for skin tissue TET applications.

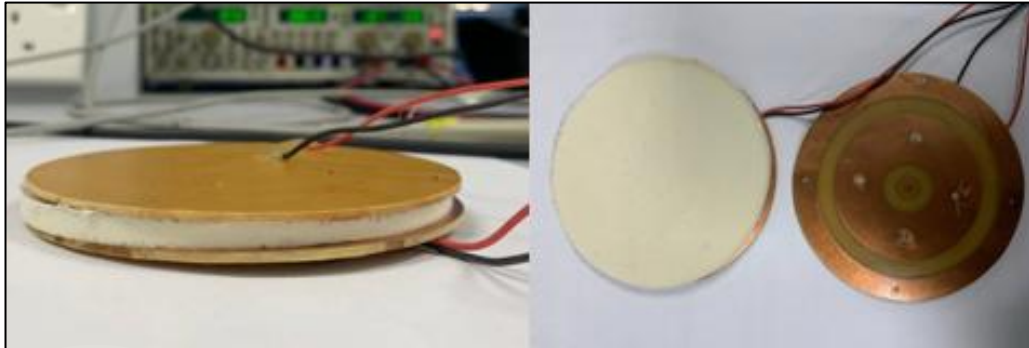


**Figure 4.12: Validation of Skin tissue**

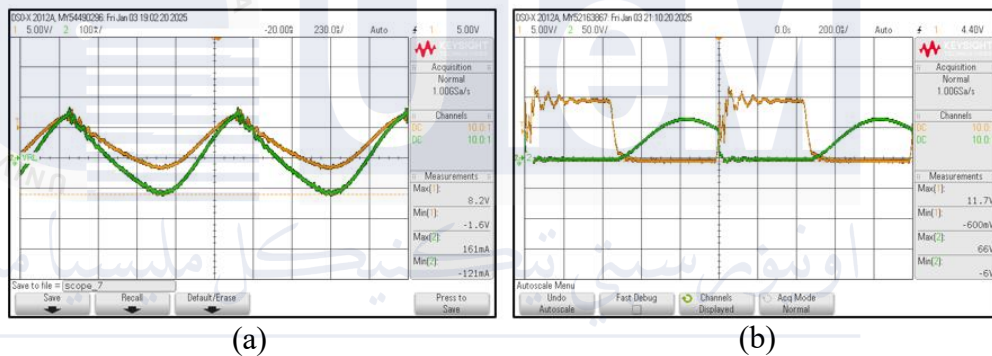


**Figure 4.13: Measurement Results for Skin Tissue (a) IV, (b) ZVS**

### 4.5.3 The Validation Process of Fat Tissue-Equivalent Phantom

For the fat tissue phantom, the validation process begins by ensuring the dielectric properties and impedance characteristics of the phantom closely resemble real human fat tissue. This is illustrated in Figure 4.14, where the validation setup confirms the compatibility of the circuit with fat tissue conditions. The IV curve, shown in Figure 4.15(a), highlights the relationship between current and voltage during the operation, providing insights into the power transfer efficiency and system behavior under fat-like material. Additionally, the validation confirms the achievement of ZVS in the circuit, as depicted in Figure 4.15(b). ZVS minimizes energy loss during switching, which is particularly important for high-frequency

applications like TET. The results validate that the circuit can effectively transfer energy through fat tissue while maintaining optimal efficiency and reliability.

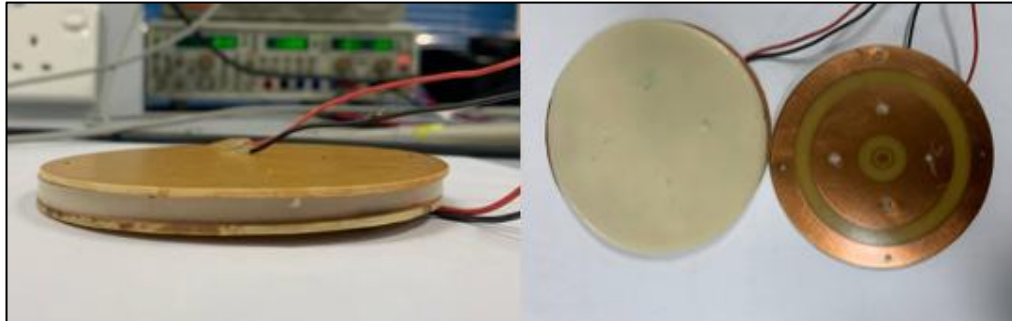
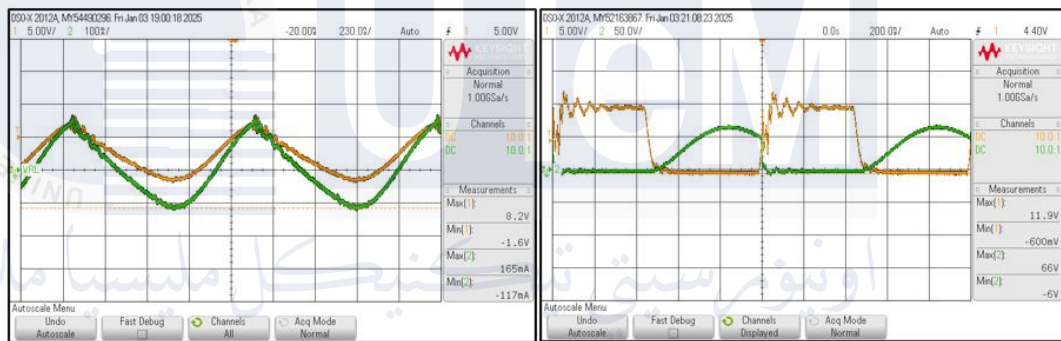


**Figure 4.14: Validation of Fat Tissue**



(a)

(b)

**Figure 4.15: Measurement Results for Fat Tissue (a) IV, (b) ZVS**

#### 4.5.4 The Validation Process of Muscle Tissue-Equivalent Phantom

The validation of the muscle tissue phantom focuses on ensuring that the circuit performs effectively when interacting with muscle-like materials. Figure 4.16 shows the validation setup, where the phantom is tested for its ability to simulate the energy transfer properties of real human muscle tissue. The IV characteristics, as seen in Figure 4.17(a), provide detailed insights into the circuit's behavior under muscle tissue conditions, highlighting its ability to maintain consistent and efficient power transfer. Finally, the ZVS performance of the circuit is validated with the muscle phantom, as shown in Figure 4.17(b). This ensures that the circuit switches with

minimal energy loss, crucial for maintaining efficiency in TET systems. The validation confirms that the system operates reliably and effectively through muscle tissue, demonstrating its potential for real-world applications in TET involving all three tissue types.

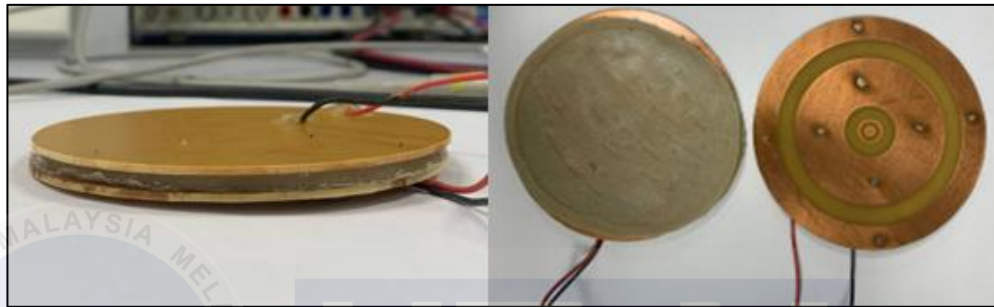


**Figure 4.16: Validation of Muscle Tissue**

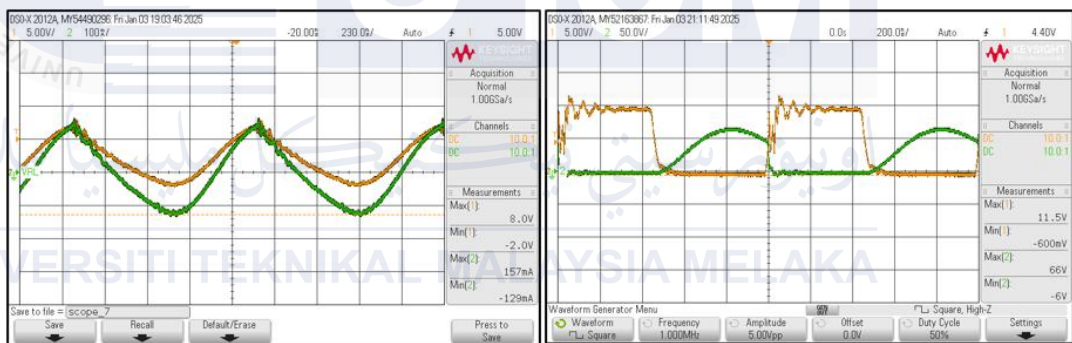


**Figure 4.17: Measurement Results for Muscle Tissue (a) IV, (b) ZVS**

## 4.6 Theoretical Validation using Transcutaneous Transfer Energy (TET) Application

### 4.6.1 Skin Tissue phantom (Using Titanium Dioxide sample)

#### a) Permittivity ( $\epsilon r$ )

The permittivity can be calculated theoretically based on the capacitance formula and the geometry of the skin tissue:

$$\epsilon r = \frac{C.d}{\epsilon_0.A} \quad (4.1)$$

Where:

- $\epsilon_0 = 8.854 \times 10^{-12} F/m$
- $d = 0.005 \text{ m (thickness)}$
- $A = \pi r^2 = \pi(0.05)^2 = 7.854 \times 10^{-3} m^2$
- $Z = \frac{V}{I} = \frac{8.2}{0.161} = 50.93 \Omega$

Capacitance is related to impedance as

$$C = \frac{1}{2\pi f Z} = \frac{1}{2\pi(1 \times 10^6)(50.93)} = 3.123 \times 10^{-9} F$$

$$\text{(Substituting); } \epsilon r = \frac{(3.123 \times 10^{-9})(0.005)}{(8.854 \times 10^{-12})(7.854 \times 10^{-3})} = 224.8$$

Theoretical Permittivity,  $\epsilon r = 224.8$

b) Conductivity ( $\sigma$ )

The conductivity is determined using:

$$\sigma = \frac{1}{R.A} \quad (4.2)$$

Where:

- $R = Z = 50.93\Omega$
- $A = 7.854 \times 10^{-3}m^2$

Substituting:  $\sigma = \frac{1}{(50.93)7.854 \times 10^{-3}} = 2.516 S/m$

Theoretical Conductivity,  $\sigma = 2.516 S/m$

c) Loss Tangent( $\tan \delta$ )

The loss tangent is calculated as:

$$\tan \delta = \frac{\sigma}{2\pi f \epsilon_0 \epsilon_r} \quad (4.3)$$

$$\tan \delta = \frac{2.516}{2\pi(1 \times 10^6)(8.854 \times 10^{-12})(224.8)} = 0.02$$

Theoretical Loss Tangent,  $\tan \delta = 0.02$

**Table 4.7: Comparison between Measured and Theoretical Values of Skin**

Dielectric Properties	Theoretical	Measured Value
Permittivity	224.8	1319.47
Conductivity	2.516 S/m	0.73 S/m
Loss Tangent	0.02	15.35

#### 4.6.2 Fat Tissue phantom (Using Fat sample F1) & Muscle Tissue phantom (Using Silver powder sample)

**Table 4.8: Comparison between Measured and Theoretical Values of Fat**

<b>Dielectric Properties</b>	Theoretical	Measured Value
<b>Permittivity</b>	229.0	176.01
<b>Conductivity</b>	0.00257 S/m	0.01 S/m
<b>Loss Tangent</b>	0.02	14.16

**Table 4.9: Comparison between Measured and Theoretical Values of Muscle**

<b>Dielectric Properties</b>	Theoretical	Measured Value
<b>Permittivity</b>	224.3	1792.99
<b>Conductivity</b>	2.497 S/m	0.10 S/m
<b>Loss Tangent</b>	0.02	48.67

### UNIVERSITI TEKNIKAL MALAYSIA MELAKA

The comparison between theoretical and measured values for skin, fat, and muscle shows significant discrepancies in dielectric properties. For skin and muscle, the measured relative permittivity values are significantly higher than the theoretical ones, while the conductivity values are much lower. The loss tangent for all tissues is drastically higher than theoretical expectations. These deviations can be attributed to several factors. The materials used in tissue-equivalent phantoms may not perfectly replicate the complex composition of biological tissues, particularly in terms of water content, ion concentration, and molecular structure. Additionally, the theoretical values are often based on simplified assumptions that fail to account for the heterogeneous and anisotropic nature of real tissues. Frequency dependency also plays a role, as the dielectric properties of tissues vary with frequency, and measured

values may not align with theoretical models. Moreover, fabrication techniques, such as the double-boiled process, might introduce inconsistencies in texture or uniformity, further impacting results. Lastly, environmental factors and measurement errors, such as equipment calibration and testing conditions, can contribute to the observed differences. These discrepancies highlight the need for improved material selection, fabrication processes, and testing protocols to achieve phantoms that more accurately replicate human tissue properties.



## CHAPTER 5

### CONCLUSION AND FUTURE WORKS



#### 5.1 Conclusion

This thesis discusses the comprehensive development of a tissue equivalent phantom for Transcutaneous Transfer Energy (TET) Application. The three types of phantoms can be mimicked and have been developed by previous researchers: solid, liquid, and semi-solid. In this project, the focus was on semi-solid types of phantoms because they are very close to human tissue structure, and they are the best for developing skin, fat, and muscle tissue phantoms. The development of tissue-equivalent phantom for Transcutaneous transfer energy (TET) Application has been done correctly to ensure the best ingredients used to mimicking the tissue phantom have a unique characteristic.

"Development of a Tissue-Equivalent Phantom for Transcutaneous Energy Transfer (TET) Application," successfully met its objectives through a systematic and interdisciplinary approach. Initially, the study identified and evaluated materials capable of closely mimicking the physical, mechanical, and electromagnetic properties of human tissues. These materials were selected for their ability to replicate the dielectric, conductivity, and structural characteristics essential for TET applications.

A functional tissue-equivalent phantom was then developed, specifically designed to operate at the critical frequencies of 1 MHz and 13.56 MHz, ensuring efficient and safe energy transmission for TET systems. The fabrication process employed innovative techniques, such as the double-boiled method, to achieve a realistic, layered structure that mimics the heterogeneous and stratified nature of human tissue. This approach ensured that the phantom's texture and uniformity met the stringent requirements for energy transfer studies. In the final phase, the phantom was rigorously characterized through comprehensive testing to validate its electromagnetic compatibility, mechanical stability, and performance under diverse conditions. The findings confirmed that the phantom accurately simulates the behavior of human tissue in TET scenarios, providing a reliable platform for testing and optimizing TET devices. Additionally, its reproducibility and consistency enhance its value as a tool for future research and development.

Overall, this project successfully developed a tissue-equivalent phantom that serves as a robust model for advancing transcutaneous energy transfer technologies. By enabling precise testing and optimization of TET systems, this phantom

contributes to the creation of more efficient, safe, and patient-friendly solutions for implantable medical devices and wireless power transfer applications.

## 5.2 Future Work

The development of tissue-equivalent phantoms for Transcutaneous Energy Transfer (TET) applications will involve a multi-faceted approach to enhance the functionality, accuracy, and clinical relevance of the phantoms. A key focus will be the optimization of phantom materials to better mimic the dielectric properties of various human tissues, such as skin, fat, and muscle, across a wide range of frequencies relevant to TET applications. This includes investigating the effects of different additives, concentrations, and fabrication techniques on the electrical and thermal properties of the phantoms. Long-term stability of the phantoms will also be a critical area of research, ensuring consistent performance over extended use and storage periods.

Additionally, the creation of multi-layered phantoms will be prioritized to simulate realistic tissue structures, accounting for the complex interactions of electromagnetic fields in heterogeneous biological environments. This step will improve the accuracy of experimental validation for TET systems. Advanced modelling techniques will also be explored to refine the simulation of energy transfer and thermal responses under various operational conditions, helping to predict and mitigate potential safety risks such as tissue overheating.

Further, research will focus on integrating phantoms with advanced TET systems that incorporate features such as dynamic load management, impedance matching, and adaptive energy transfer mechanisms. These systems will be tested using the phantoms to evaluate their efficiency, safety, and compatibility with realistic

biological conditions. This work will also extend to studying the effects of TET on tissue-equivalent phantoms under different clinical scenarios, such as varying implant depths, patient movement, and environmental interference. Collaboration with regulatory bodies and clinical researchers will ensure that the phantoms meet standards for biomedical applications and facilitate their clinical translation. To promote reproducibility and wider adoption, open-source phantom designs and methodologies will be shared with the scientific community. The scope of the research will also expand to include applications beyond TET, such as wireless implantable devices, electromagnetic imaging, and therapeutic technologies, making the phantoms a versatile tool for a range of biomedical engineering fields.

In summary, the future work aims to bridge the gap between theoretical modelling and practical implementation of TET systems by developing highly accurate, stable, and clinically relevant tissue-equivalent phantoms. This effort will not only advance TET technology but also contribute to the broader field of biomedical device research and innovation.

## REFERENCES

- [1] R. Suga, M. Inoue, K. Saito, M. Takahashi, and K. Ito, "Development of multi-layered biological tissue-equivalent phantom for HF band," *IEICE Communications Express*, vol. 2, no. 12, pp. 507–511, 2013, doi: <https://doi.org/10.1587/comex.2.507>.
- [2] A. Rakhmadi and K. Saito, "Development of 500kHz muscle equivalent solid phantom," *IEICE Communications Express*, vol. 9, no. 11, pp. 519–523, Nov. 2020, doi: <https://doi.org/10.1587/comex.2020xbl0098>.
- [3] S. TOYODA and T. YAMAMOTO, "Development of a Muscle-Equivalent Phantom for Electrical Impedance Tomography," *Nihon AEM Gakkaishi*, vol. 30, no. 2, pp. 144–149, Jan. 2022, doi: <https://doi.org/10.14243/jsaem.30.144>.
- [4] T. Slanina, Duy Hai Nguyen, J. Moll, and Viktor Krozer, "Temperature dependence studies of tissue-mimicking phantoms for ultra-wideband microwave breast tumor detection," *Biomedical physics & engineering express*, vol. 8, no. 5, pp. 055017–055017, Jul. 2022, doi: <https://doi.org/10.1088/2057-1976/ac811b>.

- [5] G. Anand, A. J. Lowe, and A. M. Al-Jumaily, "Tissue phantoms to mimic the dielectric properties of human forearm section for multi-frequency bioimpedance analysis at low frequencies," vol. 96, pp. 496–508, Mar. 2019, doi: <https://doi.org/10.1016/j.msec.2018.11.080>.
- [6] Peterson, D. M., Tell, S. G., Pham, K. D., Yu, H., Bashirullah, R., Euliano, N. R., & Fitzsimmons, J. R. (2010). A Tissue Equivalent Phantom of the Human Torso for in vivo Biocompatible Communications. In IFMBE proceedings (pp. 414–417). [https://doi.org/10.1007/978-3-642-14998-6\\_105](https://doi.org/10.1007/978-3-642-14998-6_105)
- [7] R. Aminzadeh, M. Saviz, and A. A. Shishegar, "Theoretical and experimental broadband tissue-equivalent phantoms at microwave and millimetre-wave frequencies," *Electronics Letters*, vol. 50, no. 8, pp. 618–620, Apr. 2014, doi: <https://doi.org/10.1049/el.2014.0749>.
- [8] (2007). Biological Tissue-Equivalent Phantoms Usable in Broadband Frequency Range Phantoms.
- [9] E. Lennie, C. Tsoumpas, and S. Sourbron, "Multimodal phantoms for clinical PET/MRI," *EJNMMI Physics*, vol. 8, no. 1, Aug. 2021, doi: <https://doi.org/10.1186/s40658-021-00408-0>.
- [10] T. Breslin et al., "A Novel Anthropomorphic Phantom Composed of Tissue-Equivalent Materials for Use in Experimental Radiotherapy: Design, Dosimetry and Biological Pilot Study," *Biomimetics*, vol. 8, no. 2, pp. 230–230, May 2023, doi: <https://doi.org/10.3390/biomimetics8020230>.
- [11] L. Fomundam and J. Lin, "Multi-layer low frequency tissue equivalent

phantoms for noninvasive test of shallow implants and evaluating antenna-body interaction,” PubMed, Aug. 2016, doi: <https://doi.org/10.1109/embc.2016.7591202>.

[12] A. P. Gregory, K. Quéléver, D. Allal, and O. Jawad, “Validation of a Broadband Tissue-Equivalent Liquid for SAR Measurement and Monitoring of Its Dielectric Properties for Use in a Sealed Phantom,” *Sensors*, vol. 20, no. 10, p. 2956, May 2020, doi: <https://doi.org/10.3390/s20102956>.

[13] H. Kato et al., “Composition of MRI phantom equivalent to human tissues,” *Medical Physics*, vol. 32, no. 10, pp. 3199–3208, Sep. 2005, doi: <https://doi.org/10.1118/1.2047807>.

[14] M. M. McCormick, E. L. Madsen, M. E. Deaner, and T. Varghese, “Absolute backscatter coefficient estimates of tissue-mimicking phantoms in the 5–50 MHz frequency range,” *The Journal of the Acoustical Society of America*, vol. 130, no. 2, pp. 737–743, Aug. 2011, doi: <https://doi.org/10.1121/1.3605669>.

[15] Maxim Zhadobov, Anda Guraliuc, Nacer Chahat, and Ronan Sauleau, “Tissue- equivalent phantoms in the 60-GHz band and their application to the body-centric propagation studies,” HAL (Le Centre pour la Communication Scientifique Directe), Dec. 2014, doi: <https://doi.org/10.1109/imws-bio.2014.7032417>.

[16] Maxim Zhadobov, Anda Guraliuc, Nacer Chahat, and Ronan Sauleau, “Tissue- equivalent phantoms in the 60-GHz band and their application to the body-centric propagation studies,” HAL (Le Centre pour la Communication

- Scientifique Directe), Dec. 2014, doi: <https://doi.org/10.1109/imws-bio.2014.7032417>.
- [17] M. J. Hagmann, R. L. Levin, L. Calloway, A. J. Osborn, and K. R. Foster, "Muscle- equivalent phantom materials for 10-100 MHz," *IEEE Transactions on Microwave Theory and Techniques*, vol. 40, no. 4, pp. 760–762, Apr. 1992, doi: <https://doi.org/10.1109/22.127527>.
- [18] L. K. Ryan and F. Stuart. Foster, "Tissue equivalent vessel phantoms for intravascular ultrasound," *Ultrasound in Medicine & Biology*, vol. 23, no. 2, pp. 261–273, Jan. 1997, doi: [https://doi.org/10.1016/s0301-5629\(96\)00206-2](https://doi.org/10.1016/s0301-5629(96)00206-2).
- [19] N. Chahat, M. Zhadobov, and R. Sauleau, "Broadband Tissue-Equivalent Phantom for BAN Applications at Millimeter Waves," *IEEE Transactions on Microwave Theory and Techniques*, vol. 60, no. 7, pp. 2259–2266, Jul. 2012, doi: <https://doi.org/10.1109/tmtt.2012.2195196>.
- [20] PeTA, "Experiments on Animals: Overview," PETA, 2017. <https://www.peta.org/issues/animals-used-for-experimentation/animals-used-experimentation-factsheets/animal-experiments-overview/>
- [21] "Dielectric Properties of Body Tissues: Home page," Ifac.cnr.it, 2018. <http://niremf.ifac.cnr.it/tissprop/>
- [22] C. Fontes-Candia et al., "Maximizing the oil content in polysaccharide-based emulsion gels for the development of tissue mimicking phantoms," *Carbohydrate polymers*, vol. 256, pp. 117496–117496, Mar. 2021, doi: <https://doi.org/10.1016/j.carbpol.2020.117496>.

- [23] W. M. MILLER and C. T. MORROW, “MECHANICAL CHARACTERIZATION OF FIBROUS MATERIALS AS RELATED TO MEAT ANALOGS \*\*,” *Journal of Texture Studies*, vol. 6, no. 4, pp. 473–487, Jan. 2007, doi: <https://doi.org/10.1111/j.1745-4603.1975.tb01422.x>.
- [24] L. C. Cabrelli, P. I. B. G. B. Pelissari, A. M. Deana, A. A. O. Carneiro, and T. Z. Pavan, “Stable phantom materials for ultrasound and optical imaging,” *Physics in Medicine and Biology*, vol. 62, no. 2, pp. 432–447, Jan. 2017, doi: <https://doi.org/10.1088/1361-6560/62/2/432>.
- [25] A. Arya, M. Sadiq, and A. L. Sharma, “Salt concentration and temperature dependent dielectric properties of blend solid polymer electrolyte complexed with NaPF<sub>6</sub>,” *Materials today: proceedings*, vol. 12, pp. 554–564, Jan. 2019, doi: <https://doi.org/10.1016/j.matpr.2019.03.098>.
- [26] M. Nguyen, S. Zhou, J. Robert, Vijay Shamdasani, and H. Xie, “Development of Oil-in-Gelatin Phantoms for Viscoelasticity Measurement in Ultrasound Shear Wave Elastography,” *Ultrasound in Medicine and Biology*, vol. 40, no. 1, pp. 168–176, Jan. 2014, doi: <https://doi.org/10.1016/j.ultrasmedbio.2013.08.020>.
- [27] J. Oudry, C. Bastard, V. Miette, R. Willinger, and L. Sandrin, “Copolymer-in-oil Phantom Materials for Elastography,” *Ultrasound in Medicine & Biology*, vol. 35, no. 7, pp. 1185–1197, Jul. 2009, doi: <https://doi.org/10.1016/j.ultrasmedbio.2009.01.012>.
- [28] L. Fomundam and J. Lin, “Multi-layer low frequency tissue equivalent phantoms for noninvasive test of shallow implants and evaluating antenna-

body interaction,” PubMed, Aug. 2016, doi:  
<https://doi.org/10.1109/embc.2016.7591202>.

[29] S. Ohno et al., “Production of a human-tissue-equivalent MRI phantom: optimization of material heating,” *Magnetic resonance in medical sciences: MRMS: an official journal of Japan Society of Magnetic Resonance in Medicine*, vol. 7, no. 3, pp. 131–140, 2008, doi:  
<https://doi.org/10.2463/mrms.7.131>.

[30] *N1500A*. (n.d.). <https://helpfiles.keysight.com/csg/N1500A/N1500A.htm>

[31] Schädel-Ebner, S., Hirsch, O., Gladytz, T., Gutkelch, D., Licha, K., Berger, J., & Grosenick, D. (2022). 3D-printed tissue-simulating phantoms for near-infrared fluorescence imaging of rheumatoid diseases. *Journal of Biomedical Optics*, 27(07). <https://doi.org/10.1117/1.jbo.27.7.074702>

[32] Chmarra, M. K., Hansen, R., Mårvik, R., & Langø, T. (2013). Multimodal phantom of liver tissue. *PLoS ONE*, 8(5), e64180. <https://doi.org/10.1371/journal.pone.0064180>

[33] Hatamikia, S., Jaksa, L., Kronreif, G., Birkfellner, W., Kettenbach, J., Buschmann, M., & Lorenz, A. (2023). Silicone phantoms fabricated with multi-material extrusion 3D printing technology mimicking imaging properties of soft tissues in CT. *Zeitschrift Für Medizinische Physik*. <https://doi.org/10.1016/j.zemedi.2023.05.007>

[34] Gurjar, O., Mishra, S., Bhandari, V., Pathak, P., Patel, P., & Shrivastav, G. (2014). Radiation dose verification using real tissue phantom in modern

radiotherapy techniques. *Journal of Medical Physics*, 39(1), 44. <https://doi.org/10.4103/0971-6203.125504>

[35] Rahman, M. A., Bhuiyan, M. T. H., Rahman, M. M., & Chowdhury, M. (2018). Comparative study of absorbed doses in different phantom materials and fabrication of a suitable phantom. *Malaysian Journal of Medical and Biological Research*, 5(1), 19–24. <https://doi.org/10.18034/mjmbr.v5i1.444>

[36] Dissanayake, T., Budgett, D., Hu, A. P., Malpas, S., & Bennet, L. (2009). Transcutaneous energy transfer system for powering implantable biomedical devices. In *IFMBE proceedings* (pp. 235–239). [https://doi.org/10.1007/978-3-540-92841-6\\_57](https://doi.org/10.1007/978-3-540-92841-6_57)

